Development/Plasticity/Repair

Molecular Basis of the Interactions of the Nogo-66 Receptor and Its Homolog NgR2 with Myelin-Associated Glycoprotein: Development of NgR^{OMNI}-Fc, a Novel Antagonist of CNS Myelin Inhibition

Laurie A. Robak,[5]* Karthik Venkatesh,[2]* Hakjoo Lee,[5] Stephen J. Raiker,[1,2,5] Yuntao Duan,[1,2] Jane Lee-Osbourne,[5] Thomas Hofer,[3] Rose G. Mage,[4] Christoph Rader,[3] and Roman J. Giger[1,2,5]

Departments of [1]Cell and Developmental Biology and [2]Neurology, University of Michigan School of Medicine, The University of Michigan, Ann Arbor, Michigan 48109-2200, [3]Experimental Transplantation and Immunology Branch, Center for Cancer Research, National Cancer Institute, National Institutes of Health, Bethesda, Maryland 20892-1203, [4]Laboratory of Immunology, National Institute of Allergy and Infectious Diseases, National Institutes of Health, Bethesda, Maryland 20892-1892, and [5]Department of Biomedical Genetics, School of Medicine and Dentistry, University of Rochester, Rochester, New York 14642

Myelin-associated glycoprotein (MAG) is a sialic acid-binding Ig-family lectin that functions in neuronal growth inhibition and stabilization of axon–glia interactions. The ectodomain of MAG is comprised of five Ig-like domains and uses neuronal cell-type-specific mechanisms to signal growth inhibition. We show that the first three Ig-like domains of MAG bind with high affinity and in a sialic acid-dependent manner to the Nogo-66 receptor-1 (NgR1) and its homolog NgR2. Domains Ig3–Ig5 of MAG are sufficient to inhibit neurite outgrowth but fail to associate with NgR1 or NgR2. Nogo receptors are sialoglycoproteins comprised of 8.5 canonical leucine-rich repeats (LRR) flanked by LRR N-terminal (NT) and C-terminal (CT)-cap domains. The LRR cluster is connected through a stalk region to a membrane lipid anchor. The CT-cap domain and stalk region of NgR2, but not NgR1, are sufficient for MAG binding, and when expressed in neurons, exhibit constitutive growth inhibitory activity. The LRR cluster of NgR1 supports binding of Nogo-66, OMgp, and MAG. Deletion of disulfide loop Cys^{309}–Cys^{336} of NgR1 selectively increases its affinity for Nogo-66 and OMgp. A chimeric Nogo receptor variant (NgR^{OMNI}) in which Cys^{309}–Cys^{336} is deleted and followed by a 13 aa MAG-binding motif of the NgR2 stalk, shows superior binding of OMgp, Nogo-66, and MAG compared with wild-type NgR1 or NgR2. Soluble NgR^{OMNI} (NgR^{OMNI}-Fc) binds strongly to membrane-bound inhibitors and promotes neurite outgrowth on both MAG and CNS myelin substrates. Thus, NgR^{OMNI}-Fc may offer therapeutic opportunities following nervous system injury or disease where myelin inhibits neuronal regeneration.

Introduction

Adult mammalian CNS myelin contains growth inhibitory factors that contribute to the regenerative failure of severed axons following injury (Schwab, 1993). Several myelin inhibitors have been identified and most of the attention has focused on MAG, Nogo-A, and OMgp (Filbin, 2003; Xie and Zheng, 2008).

Received Sept. 27, 2008; revised Nov. 10, 2008; accepted March 12, 2009.

This work was supported by National Institutes of Health Training Grant T32 NS07489 (L.R. and K.V.), National Research Service Award Ruth Kirschstein Fellowship F31NS049870 (K.V.), the New York State Spinal Cord Injury Research Program (R.J.G. and C.R.), the Christopher Reeve and Sam Schmidt Paralysis Foundation, the Ellison Medical Foundation, the National Alliance for Research on Schizophrenia and Depression, the Dr. Miriam and Sheldon G. Adelson Medical Foundation's Adelson Program in Neural Repair and Rehabilitation, and National Institute of Neurological Disorders and Stroke Grant NS047333 (R.J.G.). We thank R. Geary, B. Carlin, and J. J. Winters for excellent technical assistance, R. Schnaar for *Galgt1* mouse brain tissue, and R. Quarles for anti-MAG B11F7.

*L.A.R. and K.V. contributed equally to this work.

Correspondence should be addressed to Roman J. Giger, Departments of Cell and Developmental Biology and Neurology, University of Michigan School of Medicine, The University of Michigan, 109 Zina Pitcher Place, 3065 BSRB, Ann Arbor, MI 48109-2200. E-mail: rgiger@umich.edu.

J. Lee-Osbourne's present address: Cold Spring Harbor Laboratory, 1 Bungtown Road, Cold Spring Harbor, NY 11724.

DOI:10.1523/JNEUROSCI.4935-08.2009

 0270-6474/09/295768-16$15.00/0

The Nogo receptors NgR1 and NgR2 show overlapping, yet distinct, binding preferences for myelin inhibitors. Nogo-A and OMgp bind selectively and with high affinity to NgR1 (Liu et al., 2006), while MAG binds preferentially to NgR2 but also interacts with NgR1 (Giger et al., 2008). *In vitro*, *NgR1* is necessary for growth cone collapse in response to acutely presented myelin inhibitors (Kim et al., 2004; Chivatakarn et al., 2007), but is dispensable for neurite outgrowth inhibition on substrate-bound Nogo-66 (Zheng et al., 2005) or MAG or OMgp (Chivatakarn et al., 2007; Venkatesh et al., 2007; Williams et al., 2008). Mechanistically, this apparent dichotomy of the role of NgR1 in neuronal growth inhibitory responses is poorly understood. Physiological *NgR1* signaling limits experience-dependent plasticity in the visual cortex (McGee et al., 2005), and in the adult hippocampus, *NgR1* regulates activity-dependent synaptic strength and dendritic spine morphology (Lee et al., 2008). Following CNS injury, *NgR1* limits axon collateral sprouting but not long-distance regenerative growth of severed corticospinal tract fibers (Kim et al., 2004; Zheng et al., 2005; Cafferty and Strittmatter, 2006).

MAG is a member of the siglec family of sialic acid-binding Ig

lectins and uses neuronal cell-type-specific mechanisms to mediate growth inhibition. Cerebellar granule neurons (CGNs) but not dorsal root ganglion (DRG) neurons deficient for complex gangliosides are more resistant to MAG inhibition. In retinal ganglion cells (RGCs), hippocampal and DRG neurons, functional depletion of gangliosides or NgR1 alone is not sufficient to attenuate MAG inhibition. Simultaneous loss of terminal sialic acids and NgR1, however, significantly attenuates MAG inhibition (Mehta et al., 2007; Venkatesh et al., 2007). A receptor complex comprised of NgR1, Lingo-1, and p75 or TROY has been implicated in signaling Nogo-66, OMgp, and MAG inhibition of neurite outgrowth (Yiu and He, 2006). *In vitro*, p75 is important for growth inhibition of DRG neurons, but neither *p75* nor *TROY* is necessary for MAG inhibition of CGNs or RGCs (Zheng et al., 2005; Venkatesh et al., 2007). MAG-induced repulsive growth cone steering requires the presence of an arginine-glycine-aspartate (RGD)-dependent interaction with neuronal β1-integrin (Goh et al., 2008).

The ligand-binding domain (LBD) of NgR1 is composed of 8.5 canonical LRRs flanked by cysteine-rich LRR-NT and LRR-CT cap domains. The LBD harbors overlapping, yet distinct, binding pockets for Nogo, OMgp, and MAG (Schimmele and Plückthun, 2005; Laurén et al., 2007). In soluble form, the NgR1 LBD [NgR1(310)] has CNS myelin inhibitor antagonistic properties *in vitro* (Fournier et al., 2002; Liu et al., 2002; He et al., 2003; Zheng et al., 2005). Following spinal cord injury, NgR1(310)-Fc promotes sprouting and regenerative growth of severed corticospinal and raphespinal fibers (Li et al., 2004; Wang et al., 2006).

Here, we define the structural basis of the MAG association with NgR1 and NgR2 and develop a soluble chimeric Nogo receptor variant with potent CNS myelin antagonistic properties.

Materials and Methods

Recombinant DNA constructs. Chimeric receptors were generated by PCR using rat NgR1, NgR2, or NgR3 cDNA templates and assembled in the expression vector pMT21 (Venkatesh et al., 2005). To fuse PCR-amplified receptor fragments, either endogenous restriction enzyme sites or newly introduced restriction sites were used that resulted in either no amino acid substitution or conservative substitutions. None of the conserved leucine or phenylalanine residues critical for the tertiary structure of the LRR cluster or cysteine residues in the LRRNT- and LRRCT-cap domains implicated in disulfide bonds were altered. N-terminal NgR1 and NgR2 deletion mutants were fused to the signal sequence of peptidylglycine α-amidating monooxygenase (PAM) followed by a myc epitope and a five residue glycine (Gly_5)-spacer. Soluble receptor constructs were fused C-terminally to the Fc portion of human IgG1 and assembled in the expression vectors pcDNA1 or pcDNA3 (Invitrogen). Membrane-bound myc-tagged Nogo-66 (myc-Nogo-66-Npn1) was constructed by fusing human Nogo-66 to the transmembrane and cytoplasmic portion of rat neuropilin-1 in the pSecTag expression vector. Soluble full-length MAG ectodomain and deletion mutants were N-terminally fused to the PAM signal sequence, followed by a myc epitope and a Gly_5-spacer and C-terminally fused to Fc. MAG constructs were assembled in pcDNA3.0 (Invitrogen), sequenced, and analyzed by ELISA and Western blotting. Constructs included MAG(1–5)-Fc (residues S17–A506), MAG(3–5)-Fc (residues L234–A506), MAG(1–3)-Fc (residues S17–A325), and $MAG(1–3)^{R118A}$-Fc, harboring an arginine-to-alanine point mutation at residue 118. For a complete list of all NgR1 and NgR2 expression constructs generated, see supplemental Table 1 (available at www.jneurosci.org as supplemental material).

Fusion protein production and purification. Soluble fusion proteins were produced in transiently transfected HEK293T cells using Lipofectamine 2000. Conditioned cell culture supernatant (OptiMEM, Invitrogen) was collected and tumbled overnight with protein A/G beads (Merck Biosciences). After rinsing with PBS, proteins were eluted with 0.1 M glycine, pH 2.5, and dialyzed (10 kDa cutoff; Thermo Fisher Scientific) against PBS. The purity of fusion proteins was verified by SDS-PAGE followed by Coomassie staining. Before protein A/G purification, some batches of soluble receptor were preincubated with *Vibrio cholerae* neuraminidase (Sigma) (1 mU/ml) in 1 mM $CaCl_2$. Siglec3-Fc was obtained from R&D Systems. MAG(1–5)-Fc was either purchased from R&D Systems or purified from conditioned media of transiently transfected HEK293T cells.

Receptor binding studies. For ligand–receptor binding studies, COS-7 cells were plated at ~80% confluency onto poly-D-lysine (50 μg/ml, Sigma)-coated 24-well plates (Costar, 3525) and cultured overnight before transfection with NgR1 or NgR2 receptor variants, L-MAG, OMgp, or Nogo-66-Npn1 plasmid DNA using Lipofectamine 2000 (Invitrogen). The next day, COS-7 cells were rinsed with OptiMEM and incubated for 75 min with Fc-tagged fusion proteins preclustered with anti-human IgG conjugated to human placental alkaline phosphatase (AP) (Promega). Unbound fusion protein was removed by extensive rinsing with OptiMEM. Cells were then fixed with 1% formaldehyde in 60% acetone, rinsed twice in HBHA (HBS supplemented with 0.05% horse serum, 0.5% NaN_3), and rinsed once in HBS (Cellgro). Endogenous phosphatases were heat-inactivated by incubation at 65°C for 90 min. Binding of fusion proteins was visualized by developing the AP reaction with NBT/BCIP substrate (Sigma). The color reaction was stopped by rinsing wells with PBS. For some binding experiments, COS-7 cells were pretreated with VCN (10 mU/ml; Sigma) or α-2,3 neuraminidase (500 mU/ml,New England Biolabs). To confirm that COS-7 cells do not express Fc receptors endogenously, AP-Fc was used as a negative control for binding studies to untransfected cells. No binding was detected with AP-Fc at concentrations up to 50 nM.

Normalization of receptor cell surface expression. To assess cell surface expression of Nogo receptor constructs, transiently transfected COS-7 cells were immunolabeled with anti-NgR1, -NgR2, or -NgR3 polyclonal immune sera under nonpermeabilizing conditions (Venkatesh et al., 2005). Because different constructs contain different receptor fragments of variable length, cell surface receptor expression was normalized with chimeric rabbit/human monoclonal antibodies M5 (1 μg/ml), P14 (1 μg/ml), or mouse monoclonal IgG 9B11 (1 μg/ml, anti-myc, Cell Signaling Technology). M5 and P14 recognize epitopes located in the distal stalk region adjacent to the GPI anchor (Hofer et al., 2007). Antibodies were diluted in PBS in 1% horse serum as described previously (Hofer et al., 2007). Bound antibody was detected with anti-human IgG (Promega, 1 μg/ml) for M5 and P14 or anti-mouse IgG (0.75 μg/ml) for 9B11. For quantification of relative receptor cell surface expression levels, bound M5, P14, or anti-myc were detected with an anti-human or anti-mouse IgG conjugated to AP (Promega). Several receptor deletion constructs, including $NgR1^{LRRCT+stalk}$ and $NgR2^{LRRCT+stalk}$ constructs, were N-terminally myc-tagged (supplemental Table 1, available at www.jneurosci.org as supplemental material). Anti-myc staining was used to calibrate the relative binding strength of the NgR1- and NgR2-specific monoclonal IgGs M5 and P14. Cell surface expression levels of all receptor mutants was assessed with M5 or P14 under nonpermeabilizing conditions and allowed for comparison of their relative cell surface expression levels. Briefly, following incubation with M5 or P14 IgG in PBS and 1% horse serum, cells were rinsed three times with PBS. For quantification of bound antibody, cells were lysed in 10 mM HEPES, pH 7.0, and 0.1% Triton X-100 at 65°C for 2 h. The AP activity in lysates was quantified with a Microplate Reader (Bio Tek Instruments) by measuring the absorption at 415 nm. For each receptor construct, ligand binding was normalized to cell surface receptor expression levels.

Quantification of binding. The relative strength of protein–protein interactions was measured as described previously (Venkatesh et al., 2005). Relative binding affinities to receptor variants were normalized to receptor surface expression and plotted against AP-Nogo-66 binding to wild-type NgR1 (100%), OMgp-AP binding to wild-type NgR1 (100%), or binding of oligomerized MAG-Fc to NgR1 (100%). Binding of soluble NgR1-Fc to membrane-bound L-MAG, OMgp, and Nogo-66-Npn1 was each set to 100% and used for normalization of relative binding strength and comparison to the fusion proteins NgR1(310)-Fc, NgR2-Fc, NgR^{OMNI}-Fc, $NgR2^{LRRCT+stalk}$-Fc, or AP-Fc. MAG(1–5)-Fc, MAG(1–

3)-Fc, MAG(1–3)^{R118A}-Fc, and MAG(3–5)-Fc binding to NgR1, NgR2, and MAG was quantified using Microsuite Five (Olympus) quantification software. For this method, COS-7 cells were not lysed, but were fixed onto the plate, heat inactivated at 65°C, and developed in NBT/BCIP substrate. Black and white images were taken with a CC-12 CCD camera attached to an IX71 Olympus microscope. Pixel intensity of 30–50 cells with positive binding was compared with pixel intensity of adjacent cells with no binding. Comparison of the digital imaging method (Microsuite Five software) and the cell lysis method (Venkatesh et al., 2005) to quantify ligand binding yielded similar results.

Analysis of NgR1 and NgR2 glycosylation in neural tissue. Rat P7 forebrain homogenate (50 μg) was treated with VCN (10 mU/mg) for 1 h at 37°C in a reaction buffer containing 5 mM sodium acetate and 1 mM $CaCl_2$, pH 5.5. For double digestion with PNGase F, VCN-treated samples were denatured by boiling for 10 min in 0.5% SDS and 40 mM DTT. Samples were then digested with 3 μl of PNGaseF (500 U/ml; New England Biolabs) in 1% NP-40, 50 mM sodium phosphate, pH 7.5, for 1 h at 37°C. Adult brains of *Galgt1* heterozygous (+/−) and mutant (−/−) mice were kindly provided by R. Schnaar (Johns Hopkins University, Baltimore, MD). The neocortices from *Galgt1* (+/−) and (−/−) brains were dissected and lysed in modified RIPA buffer (50 mM Tris HCl, 150 mM NaCl, 1% NP-40, 1 mM $MgCl_2$, and 0.25% sodium deoxycholate) and incubated with or without VCN (10 mU/mg) and protease inhibitor mix (Sigma) for 1 h at 37°C. The reaction was stopped by incubation in Laemmli buffer/β-mercaptoethanol. Following boiling, protein samples were separated by SDS-PAGE and blotted on polyvinyl membranes. Mouse NgR1 and NgR2 were detected with a goat anti-NgR1 or anti-NgR2 immune serum.

For two-dimensional (2-D) gel electrophoresis, we used Triton X-100-insoluble lipid raft fractions isolated from P14 rat brain extracts by flotation in a sucrose gradient as described previously (Venkatesh et al., 2005). A total of 50 μg of lipid raft protein was subjected to 2-D gel electrophoresis in a pH gradient of 4–9.5 (Kendrick Labs). For Western blotting, the membrane was probed with a polyclonal rabbit anti-NgR1 immune serum (Venkatesh et al., 2005) followed by anti-caveolin (22 kDa) as a marker for lipid rafts.

ELISA of soluble MAG fusion proteins. Goat anti-human IgG (10 μg/ml; Millipore Bioscience Research Reagents) was used to coat 96-well ELISA plates (BD Biosciences) overnight at 4°C. After rinsing with PBS, Fc-tagged MAG deletion constructs were applied, incubated for 2 h at 37°C, rinsed in PBS, and blocked in 1% BSA in PBS for 1 h at room temperature. Anti-MAG 513 antibody (Millipore Bioscience Research Reagents) was applied overnight at 4°C, wells were rinsed and then incubated with AP-conjugated anti-mouse Fc (Promega) for 1 h at room temperature. Bound AP activity was quantified using a Microplate Reader (Bio Tek Instruments) to measure absorption at 415 nm.

Myelin preparation. Spinal cord myelin was isolated from 2 to 3 months old female Sprague Dawley rats using a modified version of the method described by Colman et al. (1982). Briefly, spinal cords from 5 rats were dissected (2.1 g) and homogenized in 21 ml of ice-cold low-sucrose buffer [0.25 M sucrose, 10 mM HEPES pH 7.4, 3 mM DTT, 5 mM EDTA, and 210 μl of tissue protease inhibitor mix (Sigma)]. The tissue homogenate was centrifuged at 4°C for 2 min at 1000 rpm (Beckman, Allegra 6R) and the supernatant was stored on ice. The pellet was homogenized in 10 ml of low-sucrose buffer and centrifuged as described. The resulting pellet (P1) was frozen and the combined supernatants (25 ml, SN1) were adjusted to 1.4 M sucrose by adding 55 ml of ice-cold high sucrose buffer (1.9 M sucrose, 10 mM HEPES pH 7.4, 3 mM DTT, 5 mM EDTA, and 1:200 protease inhibitor mix). In a 36 ml centrifuge tube (Sorvall 630/36 rotor tubes), 28 ml of spinal cord extract were overlaid with 5 ml of ice-cold 0.85 M sucrose buffer (0.85 M sucrose, 10 mM HEPES pH 7.4, 3 mM DTT, 5 mM EDTA, and 1:200 protease inhibitor) and 3 ml of 0.25 M low-sucrose buffer and then spun for 1 h at 75,000 × *g* (Sorval swing-out rotor 630; 20,000 rpm). Myelin was enriched and collected from the 0.25/0.85 sucrose interphase (M1). Microsomes and polysomes were collected at the 0.85/1.4 M sucrose interphase (M2). M1 and M2 were each diluted 1:10 in ice-cold 10 mM HEPES, pH 7.4, homogenized on ice, and spun for 20 min at 75,000 × *g* (first osmotic shock). The pellets were resuspended in 10 mM HEPES, homogenized, and centrifuged as described. The osmotic step was repeated once. The pellets were resuspended in 10 mM HEPES and the protein concentration (pellet P3 = microsomes/polysomes and pellet P4 = myelin membranes) was determined using the Pierce protein concentration method. Western blot analysis with anti-MAG (B11F7, 1:1000 mouse monoclonal Ab, kindly provided by R. Quarles, National Institutes of Health/National Institute of Neurological Disorders and Stroke, Bethesda, MD), anti-NogoA/B and anti-OMgp (1:1000 goat polyclonal Abs, R&D Systems), anti-MBP (1:1000 mouse monoclonal Ab, Covance), and anti-tubulin (Sigma, 1:2000 mouse) were done on microsome/polysome and myelin fractions to assess the quality of the prepared myelin and the relative distribution of inhibitors among the two fractions (supplemental Fig. S8, available at www.jneurosci.org as supplemental material). The myelin fractions were aliquoted and stored at −80°C. For functional assays, membrane proteins of fraction P4 were extracted with 1% CHAPS buffer for 4 h at 4°C before centrifugation to remove nonsoluble proteins.

Affinity precipitation. Myelin membranes (1 mg) were lysed in buffer containing 20 mM Tris-HCl, pH 7.5, 150 mM NaCl, 5 mM EDTA, and 1% CHAPS overnight at 4°C with tumbling. Following centrifugation at 14,000 rpm for 10 min to remove insoluble material, lysates were tumbled for 4 h at 4°C in the presence of 0.5% BSA and protease inhibitor in the presence of 5 μg of NgR^{OMNI}-Fc, NgR1(310)-Fc, NgR2$^{LRRCT+stalk}$-Fc, or anti-MAG 513 antibody or control IgG. Protein G Plus/protein A-agarose beads (Merck Biosciences) were added and tumbled at 4°C for 2 h. Affinity precipitation was performed as described previously (Lee et al., 2008), and precipitates were analyzed by SDS-PAGE and immunoblotting with anti-MAG B11F7 (generous gift from R. Quarles). Recombinant OMgp (R&D Systems) was used for affinity precipitation experiments with soluble Nogo receptor fusion proteins

Neurite outgrowth assay. Glass coverslips (Propper) were acid etched, rinsed in 100% ethanol, and dried thoroughly before being placed in 24-well plates. Nitrocellulose (1 cm^2) was dissolved in methanol (1 ml), coated onto acid-etched glass coverslips, and dried completely. MAG(1–5)-Fc (R&D Systems), Siglec3-Fc (R&D Systems), bovine serum albumin (BSA), or rat spinal cord myelin membranes dissolved in 1% CHAPS was adsorbed onto the nitrocellulose-coated glass coverslips at ambient temperature for 1 h. Protein was coated at specified concentrations (see Results for details) and wells never dried. Unbound soluble protein was rinsed off with PBS before addition of poly-D-lysine (Sigma) at 100 μg/ml for 1 h. After rinsing, the wells were coated with laminin (1.5 μg/ml; Invitrogen) for 1 h for postnatal rat CGN cultures. Percoll-purified P7–P8 rat CGNs were prepared concurrently (Venkatesh et al., 2005), plated at a concentration of 65,000 per well, and cultured for 16 h before fixation in 4% paraformaldehyde. For E18 rat cortical neurons, fibronectin (5 μg/ml; EMD Biosciences) was used in place of laminin. E18 rat cortical neurons were prepared as described previously (Lee et al., 2008), plated at a concentration of 50,000 neurons per well, and fixed after incubating for 21 h. For experiments with soluble receptor fusion proteins, equal volumes of Ig-purified soluble proteins were added to wells immediately following plating of neurons for a final concentration of 10 μg/ml. For dose–response experiments, neurons were plated on a constant amount of substrate-adsorbed MAG(1–5)-Fc (2 μg/well), and increasing concentrations of NgR^{OMNI}-Fc, NgR2$^{LRRCT+stalk}$-Fc, or NgR1(310)-Fc (0–20 μg/ml) were added to the culture medium.

For transfection of P7–P8 CGNs the Amaxa nucleofection method was used as described previously (Venkatesh et al., 2005). Briefly, CGNs were purified in a discontinuous Percoll gradient and cultured in Neurobasal medium with 1× B27 supplement, 25 mM glucose, 1 mM glutamine, and Pen/Strep. For transfection, 5–7 × 10^6 CGNs in 100 μl of Nucleofector kit V solution were mixed with 4 μg of pEGFP plasmid DNA or a mixture of 3 μg of NgR1(LRRCT+stalk) and 1 μg of pEGFP or 3 μg of NgR2(LRRCT+stalk) and 1 μg of pEGFP using the O-03 pulsing parameter. Following transfection, CGNs were plated onto confluent monolayers of CHO or CHO-MAG feeder cells and cultured for 20 h. Cells were then fixed and stained by anti-GFP and anti-βIII-tubulin (TuJ1, Promega) double immunofluorescence, and neurite length was quantified as described previously (Venkatesh et al., 2005).

Quantification of neurite length and statistical analysis. Following fixation, neuronal cultures were immunostained with TuJ1. Nine images in

the center of each well were acquired at a magnification of 10× using an Olympus IX71 inverted microscope (Olympus) equipped with a DP70 digital camera. Length of neurites approximately equal to or greater than one cell body in diameter was assessed using the UTHSCSA ImageTool for Windows (Venkatesh et al., 2005). For each condition, between 15 and 350 neurites were counted per assay. All experiments were repeated independently three to five times. For statistical analysis, GraphPad Prism IV was used (unpaired *t* test). All error bars shown indicate SEM.

Results

The first three Ig-like domains of MAG are sufficient for high-affinity NgR1 and NgR2 binding

The MAG ectodomain is composed of five Ig-like domains (Ig1–5), with the lectin activity located toward the N-terminal Ig-like domains (Fig. 1). Previous studies revealed that a deletion mutant composed of the first three Ig-like domains, MAG(1–3)-Fc, binds strongly and in a sialic acid-dependent manner to the surface of neurons and neuron-like cells (Strenge et al., 1999). The MAG inhibition site can be dissociated from the sialic acid binding site (Tang et al., 1997) and has recently been mapped to Ig5 (Cao et al., 2007). To examine the structural basis of MAG binding to NgR1 and NgR2, we generated the soluble MAG ectodomain deletion mutants MAG(1–3)-Fc and MAG(3–5)-Fc, comprised of the first three Ig-like domains and the last three Ig-like domains, respectively. NgR1 and NgR2 expressed on the surface of COS-7 cells support binding of oligomerized MAG(1–3)-Fc comparable to MAG(1–5)-Fc (Fig. 1). Neither MAG(1–5)-Fc nor MAG(1–3)-Fc binds to mock-transfected COS-7 cells (supplemental Fig. S3, available at www.jneurosci.org as supplemental material). Interestingly, MAG(3–5)-Fc, containing the growth inhibitory site(s) of MAG, fails to complex with NgR1 or NgR2.

The MAG lectin activity is located within domains Ig1–3 (Kelm et al., 1994). To assess the contribution of sialic acids for MAG binding to NgR1 and NgR2, we generated MAG(1–3)^{R118A}-Fc, a point mutant with greatly decreased lectin activity (Tang et al., 1997; Vinson et al., 2001). As shown in Figure 1, MAG(1–3)^{R118A}-Fc binding to NgR1 and NgR2 is greatly reduced compared with MAG(1–3)-Fc. Proper folding of MAG(1–3)^{R118A}-Fc was confirmed by ELISA with the conformation-specific anti-MAG antibody 513 (Meyer-Franke et al., 1995) (supplemental Fig. S1, available at www.jneurosci.org as supplemental material). As an independent control for the integrity of the MAG(1–3)^{R118A}-Fc and MAG(3–5)-Fc fusion proteins, we show that they both participate in MAG homophilic binding (supplemental Fig. S2, available at www.jneurosci.org as supplemental material).

The MAG lectin activity preferentially binds to α2,3-linked terminal sialic acids fused to galactose (NeuAcα2–3Galβ1–3GalNAc) (Yang et al., 1996; Collins et al., 1997; Schnaar et al., 1998). To assess whether α2,3-linked terminal sialic acids on Nogo receptors contribute to MAG binding, NgR1- and NgR2-expressing COS cells were preincubated with α2,3-specific neuraminidase. Following enzyme treatment, MAG(1–3)-Fc binding to NgR1 is reduced by 52 ± 4% and binding to NgR2 is reduced by 61 ± 2% (Fig. 1*C*,*D*). Importantly, Nogo-66 binding to NgR1 is not sialic acid dependent (supplemental Fig. S3, available at www.jneurosci.org as supplemental material). In summary, our results reveal that the first three Ig-like domains of MAG are sufficient to confer sialic acid-dependent binding of NgR1 and NgR2. When coupled with the observation that MAG(3–5)-Fc fails to complex with NgR1 and NgR2, this suggests that Ig3 is not sufficient and that Ig1 and Ig2 are necessary for NgR1 and NgR2 binding. Consistent with the idea that the Nogo receptor binding site is located in the first two Ig-like domains of MAG, arginine 118 (R118), located in Ig1 of MAG, is important for NgR1 and NgR2 binding. Of interest, R118 is also part of the arginine-glycine-aspartate (RGD) motif of MAG, previously shown to be essential for β1-integrin binding and growth cone steering (Goh et al., 2008). In addition, MAG binds in a sialic acid-dependent manner to several gangliosides, including GT1b and GD1a (Collins et al., 1997). The association of MAG with gangliosides is greatly reduced following mutation of R118 (Vinson et al., 2001). Thus, we conclude that residue R118 of MAG is critical for the interaction with gangliosides, β1-integrin(s), NgR1 and NgR2.

The bulk of MAG inhibitory activity is associated with MAG(3–5)-Fc

Because construct MAG(3–5)-Fc fails to bind to NgR1 and NgR2, we assessed its ability to inhibit neurite outgrowth of P7–P8 cerebellar granule neurons (CGNs). Similar to substrate-adsorbed MAG(1–5)-Fc, MAG(3–5)-Fc is sufficient to inhibit neurite outgrowth (Fig. 1). Compared with neurite length of control CGN cultures, substrate adsorbed MAG(1–5)-Fc and MAG(3–5)-Fc lead to a significant inhibition of neurite length ($p < 0.001$). When cultured on MAG(1–3)-Fc substrate, a trend toward decreased neurite length was observed (89.5% of control), however outgrowth was not significantly decreased ($p = 0.24$) compared with control CGN cultures (Fig. 1*E*). Thus, our results with purified MAG ectodomain deletion constructs are in agreement with a previous study using MAG mutants stably expressed on the surface of CHO feeder cells (Cao et al., 2007). Because MAG(3–5)-Fc is sufficient to inhibit neurite outgrowth but does not directly bind to NgR1 or NgR2, we examined whether it binds to any of the previously identified components of the neuronal MAG receptor complex. However when ectopically expressed in COS-7 cells, neither p75 nor Troy, nor Lingo-1, supports binding of MAG(3–5)-Fc (data not shown). Because MAG binding to β1-integrin and gangliosides depends on its lectin activity (Vinson et al., 2001; Goh et al., 2008), MAG(3–5)-Fc is not expected to bind to β1-integrins or GT1b. Together, these results imply the existence of a novel, as yet unidentified neuronal binding partner for the MAG inhibitory site located in domains Ig3–5.

Nogo receptors are *N*- and *O*-linked sialoglycoproteins

The molecular basis of sialic acid-dependent binding of MAG to NgR1 and NgR2 is not well understood. NgR1 and NgR2 from rat brain lysates undergo a *V. cholerae* neuraminidase (VCN)-dependent molecular weight drop of 2–3 kDa (Venkatesh et al., 2005). This may either be due to loss of several terminal sialic acid moieties (each ~0.3 kDa) covalently linked to NgRs, or loss of an association with a MAG-binding ganglioside (~2 kDa). A recent study using analytical ultracentrifugation found that NgR1 forms a complex with GT1b (Williams et al., 2008). To more directly address whether the observed VCN-dependent drop in molecular weight of NgR1 or NgR2 is due to loss of an interaction with complex gangliosides, we analyzed the size of NgR1 and NgR2 from brain lysates of β-1,4-*N*-acetylgalactosaminyltransferase (*Galgt1*) mutant mice which lack complex gangliosides including the MAG ligands GD1a and GT1b (Kawai et al., 2001). In wild-type brain lysates, NgR1 and NgR2 migrate at an apparent molecular weight of 65 kDa (Chivatakarn et al., 2007). Western blotting revealed no difference in the molecular weight of NgR1 and NgR2 from *Galgt1* heterozygous and mutant mice. Importantly, following VCN treatment, a ~3 kDa drop in molecular weight for NgR1 and NgR2 was observed in neocortical extracts of *Galgt1* heterozygous and mutant mice (Fig. 2*A*). This demonstrates that

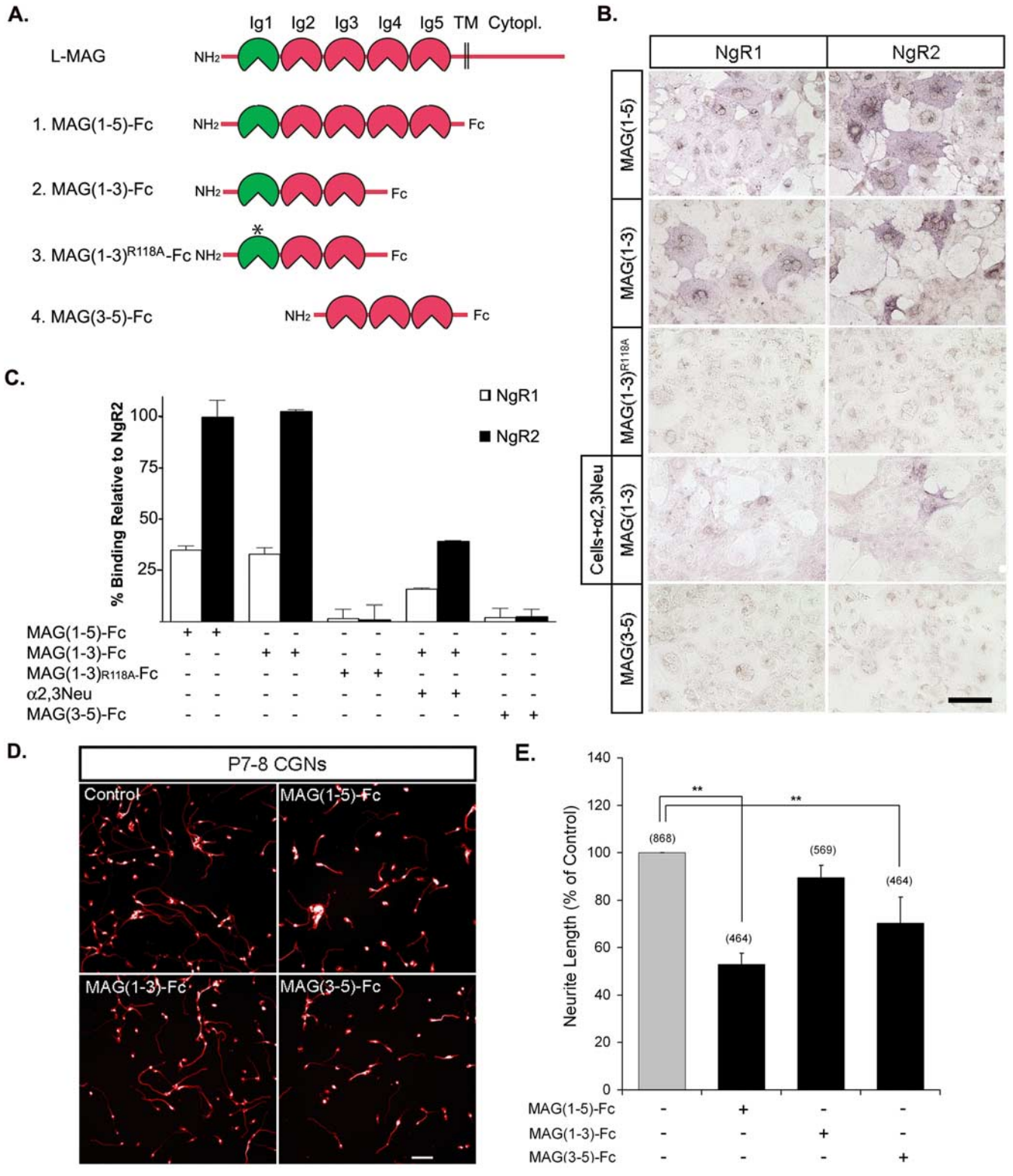

Figure 1. The first three Ig-like domains of MAG are sufficient for binding of NgR1 and NgR2 but fail to inhibit neurite outgrowth. ***A***, Schematic of MAG deletion mutants: L-MAG is composed of five Ig-like domains (Ig1-Ig5), a transmembrane (TM), and a cytoplasmic region. Domain Ig1 (shown in green) contains arginine 118 (R118), a residue important for MAG lectin activity. The point mutation R118A is labeled with an asterisk. ***B***, Binding of MAG-Fc fusion proteins to NgR1 and NgR2 expressed in COS-7 cells. MAG(1–5)-Fc and MAG(1–3)-Fc bind strongly to NgR1 and NgR2. MAG(3–5)-Fc does not bind to NgR1 or NgR2. The R118A mutation in MAG(1–3)^{R118A}-Fc virtually abolishes binding to NgR1 and NgR2. Pretreatment of NgR1- or NgR2-expressing COS-7 cells with α2,3-neuraminidase (α2,3Neu) greatly attenuates binding of MAG(1–3)-Fc. ***C***, Quantification of receptor binding of MAG ectodomain constructs in relative AP units normalized to cell surface NgR1 (white bars) and NgR2 (black bars). Binding of MAG(1–5)-Fc to NgR2 was set equal to 100%. ***D***, Neurite outgrowth inhibition assay. Substrate adsorbed MAG(3–5)-Fc, but not MAG(1–3)-Fc, is sufficient to significantly inhibit neurite outgrowth of P7–P8 cerebellar granule neurons (CGNs). ***E***, Quantification of neurite length. The number of neurites measured for each condition is indicated in parentheses. Results are presented as the mean ± SEM from three independent experiments. $^{**}p < 0.001$, significant different neurite length compared with control CGNs grown in the absence of MAG (gray bar), unpaired *t* test. Scale bars: ***B***, 30 μm; ***D***, 50 μm.

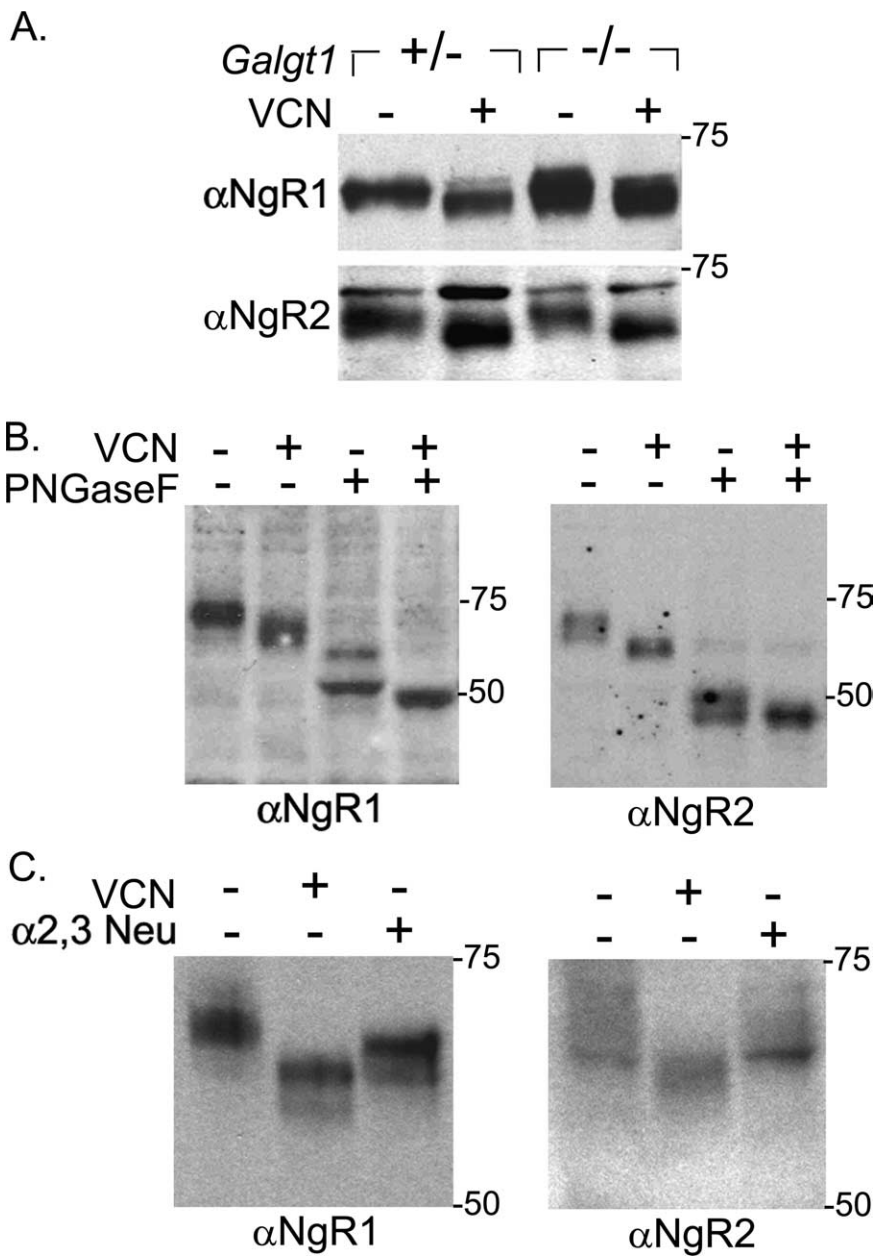

Figure 2. NgR1 and NgR2 are sialoglycoproteins that carry terminal sialic acid moieties on *N*- and *O*-linked glycan structures. ***A***, Neuraminidase treatment of cortical lysates of adult *Galgt1* heterozygous (+/−) and mutant mice (−/−) revealed a *Vibrio cholerae* neuraminidase (VCN)-dependent 2–3 kDa decrease in molecular weight of NgR1 and NgR2. ***B***, Lysates of P7 rat cortex were treated with VCN in the presence or absence of PNGaseF. Immunoblotting with anti-NgR1 or anti-NgR2 revealed a decrease of 2–3 kDa in the presence of VCN. Following PNGaseF treatment alone, two distinct immunoreactive bands were observed for both NgR1 (~58 and 52 kDa) and NgR2 (~51 and 48 kDa). A single band with an apparent molecular weight of 50 kDa for NgR1 and 48 kDa for NgR2 is observed following digestion with both enzymes. ***C***, NgR1 in rat cortical lysates treated with α2,3-neuraminidase (α2,3Neu) shows a 1–2 kDa drop in molecular weight. The drop in molecular weight for NgR2 is more subtle, but there is a decrease in the amount of higher molecular weight bands in the NgR2 lane, indicating that some sialic acids moieties on NgR2 are α2,3-linked.

the drop in molecular weight is not due to loss of an association with complex brain gangliosides.

Similar to experiments with recombinant NgR1 expressed in SH-SY5Y cells (Walmsley et al., 2004), treatment of brain lysates with PNGaseF results in a molecular weight drop and appearance of two discrete NgR1 immunoreactive bands migrating at ~58 and 52 kDa. For NgR2, two discrete species of immunoreactive bands are detected, running at ~51 and 48 kDa. The combined treatment with PNGaseF and VCN results in an additional decrease in molecular weight. A single band with an apparent molecular weight of 50 kDa for NgR1 and 48 kDa for NgR2 is observed (Fig. 2*B*). This suggests that in mouse brain tissue, the sialylation patterns for NgR1 and NgR2 are not uniform and at least two discrete sialylation patterns can be detected for each receptor. Following PNGaseF treatment, a VCN-dependent shift in molecular weight is still observed, suggesting that NgR1 and NgR2 carry sialic acid moieties on *O*-linked glycostructures. Because the VCN-dependent molecular weight shift for PNGaseF digested NgR1 and NgR2 is less robust, this also suggests that at least some terminal sialic acid moieties reside on *N*-glycans. Characteristic for many glycoproteins, 2-D gel electrophoresis of rat brain extracts revealed 15 different isoelectric variants for NgR1 within a pI range of 6–8.5 (supplemental Fig. S4, available at www.jneurosci.org as supplemental material).

Incubation of brain lysates with an α2,3-neuraminidase revealed a 1–2 kDa drop in the molecular weight for NgR1. No obvious drop in the molecular weight for NgR2 was observed; however, some of the higher molecular weight species of NgR2 are less abundant following α2,3-neuraminidase treatment (Fig. 2*C*). When coupled with the finding that MAG(1–3)-Fc binding to NgR1 and NgR2 is α2,3-neuraminidase sensitive (Fig. 1), this suggests that NgR1 and NgR2 carry a small number of MAG-binding α2,3-linked terminal sialic acid residues. In summary, NgR1 and NgR2 show complex and heterogeneous sialylation patterns. Both receptors carry terminal sialic acid moieties on *N*-linked and *O*-linked glycoconjugates, at least some of which participate in MAG binding.

The LRRs of NgR2 are dispensable for MAG binding

The three Nogo receptor family members have an identical overall domain organization and show a high degree of sequence conservation throughout the LRR cluster (composed of the LRRNT-LRR-LRRCT domains). A proline- and serine/threonine-rich stalk domain connects the LRR cluster to a glycosylphosphatidylinositol (GPI) anchor. The stalk domain of the three receptors is more variable and shows little sequence conservation (Barton et al., 2003). The crystal structure of the NgR1 LRR cluster has been resolved, revealing an elongated and arc-shaped superstructure with intramolecular disulfide bonds formed between Cys^{264}–Cys^{287} and Cys^{266}–Cys^{309} of the LRRCT-cap domain (Barton et al., 2003; He et al., 2003). In full-length NgR1, an alternate disulfide-pairing pattern was identified. Cys^{266} is linked to Cys^{335} and Cys^{309} is linked to Cys^{336} (Wen et al., 2005).

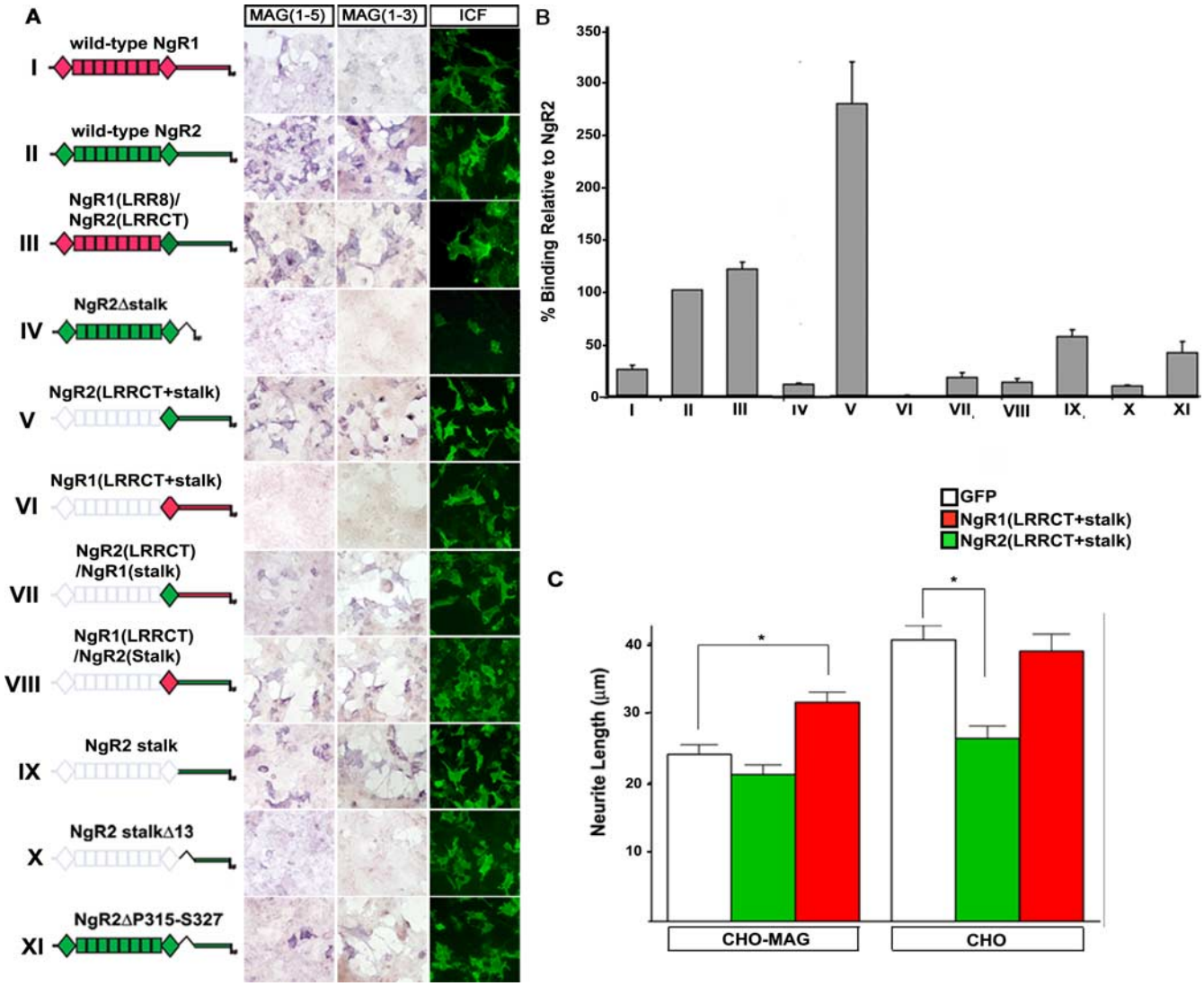

Figure 3. The minimal MAG receptor NgR2$^{LRRCT+stalk}$ is constitutively active in primary neurons. ***A***, NgR1 (red) and NgR2 (green) receptor mutants were transiently expressed in COS-7 cells. Cell surface receptor expression was confirmed by immunocytofluorescence (ICF) with the monoclonal antibodies M5 and P14 under nonpermeabilizing conditions. Binding of MAG(1–5)-Fc and MAG(1–3)-Fc, oligomerized with anti-human Fc conjugated to AP, was detected indirectly by AP enzymatic activity. The deletion mutant NgR2$^{LRRCT+stalk}$ (construct V) is sufficient to support high-affinity MAG binding, exceeding the binding strength of wild-type NgR2. Remarkably, the NgR2 stalk is sufficient to support MAG binding (construct IX) and most of its binding activity appears to reside with the proximal stalk region (construct X). None of the constructs examined showed preferential binding of MAG(1–5)-Fc over MAG(1–3)-Fc. ***B***, Quantification of MAG(1–5)-Fc binding in relative AP units. Constructs V and VI are N-terminally myc-tagged and anti-myc staining was used to calibrate the relative binding strength of the NgR1- and NgR2-specific IgGs M5 and P14. Binding to wild-type NgR2 was set equal to 100%. Error bars represent SEM from at least three independent experiments. ***C***, Quantification of neurite length of P7 CGNs transfected with receptor deletion constructs. CGNs transfected with eGFP (white bars) are strongly inhibited when cultured on CHO-MAG feeder cells and extend significantly longer neurites ($p < 0.05$) when cultured on control CHO feeder cells. Overexpression of NgR2$^{LRRCT+stalk}$ (green, construct V) results in neurite outgrowth inhibition in the absence of MAG. Conversely, overexpression of NgR1$^{LRRCT+stalk}$ (red, construct VI) in CGNs leads to a significant attenuation of MAG inhibition. Neurite length was measured from four independent assays; >100 neurites were measured per condition for each assay. *$p < 0.05$, significantly different from neurons grown on control substrate (unpaired *t* test). Error bars are in SEM. Scale bar, 30 μm.

We previously reported that MAG binds NgR2 with greater affinity than NgR1 (Venkatesh et al., 2005). Initially, to identify epitopes within NgR2 that may contribute to enhanced MAG binding, we generated chimeric Nogo receptor variants in which specific domains between NgR1 and NgR2 were swapped. For all receptor mutants, cell surface expression was assessed under nonpermeabilizing conditions and normalized with anti-NgR1- and anti-NgR2-specific mAbs (M5 and P14), which bind to an epitope in the stalk region of NgR1 or NgR2, respectively (Hofer et al., 2007) (Fig. 3*A*). MAG binding to chimeric receptors was compared with wild-type NgR2, which was arbitrarily set to 100% (Fig. 3*B*). Because MAG(1–5)-Fc binds to NgR1 and NgR2 similar to MAG(1–3)-Fc (Fig. 1), we used both ligand constructs to ask whether receptor mutants can be identified that show preferential binding of MAG(1–5)-Fc over MAG(1–3)-Fc.

Consistent with our previous observations, oligomerized MAG(1–5)-Fc binds substantially stronger to NgR2 (100%) than to NgR1 (24 ± 4%) (Venkatesh et al., 2005). A chimeric receptor comprised of the NgR1 LRRNT-cap and LRR$_{(1-8.5)}$ domains fused to the NgR2 LRRCT-cap and stalk domains (NgR1^{LRR8}/NgR2^{LRRCT}) binds MAG strongly (120 ± 7%), exceeding the avidity of wild-type NgR2 (Fig. 3). Deletion of the NgR2 stalk region (NgR2$^{\Delta stalk}$) reduces MAG binding to 11.6 ± 3% (Venkatesh et al., 2005). Remarkably, deletion of the LRRNT-cap and LRR$_{1-8.5}$ domains of NgR2, resulting in NgR2$^{LRRCT+stalk}$, does not impair MAG binding. Compared with wild-type NgR2, MAG

binding to NgR2$^{LRRCT+stalk}$ (277 ± 40%) is enhanced (Fig. 3). The strong association of MAG with NgR2$^{LRRCT+stalk}$ (residues 264–420) is in marked contrast to NgR1$^{LRRCT+stalk}$ (residues 263–473), a corresponding construct of NgR1, which fails to support MAG binding. Together, these results confirm and expand our previous observation that the structural basis of the NgR1– and NgR2–MAG association is very different. Furthermore, we identified the deletion mutant NgR2$^{LRRCT+stalk}$ as the minimal NgR2 fragment capable of conferring high-affinity MAG binding.

Identification of distinct MAG binding sites in the NgR2 LRRCT-cap and stalk

To further dissect the molecular basis of NgR2$^{LRRCT+stalk}$ (construct V) mediated MAG binding, we took advantage of the observation that NgR1$^{LRRCT+stalk}$ (VI) does not support MAG binding. This allowed the generation of chimeric receptor deletion constructs in which the LRRCT-cap domains of NgR1$^{LRRCT+stalk}$ and NgR2$^{LRRCT+stalk}$ were swapped resulting in constructs (VII) NgR2^{LRRCT}/NgR1^{stalk} and (VIII) NgR1^{LRRCT}/NgR2^{stalk} (Fig. 3*A*). When expressed on the surface of COS-7 cells, both chimerae support MAG binding weakly. Compared with wild-type NgR2, MAG binding to NgR2^{LRRCT}/NgR1^{stalk} and NgR1^{LRRCT}/NgR2^{stalk} is reduced to 17 ± 5% and 12 ± 4% (Fig. 3*B*). This suggests that the LRRCT-cap and stalk domains of NgR2 harbor distinct and dissociable MAG docking sites, both of which are necessary for high-affinity MAG binding. Because of the comparably weak binding to both chimeric receptors, it is conceivable that the two MAG binding sites of NgR2 function cooperatively to generate a high-affinity MAG-NgR2 recognition complex. Alternatively, because Cys^{335} and Cys^{336} of NgR1 are not conserved in NgR2, disulfide bonds formed between the LRRCT-cap domain and proximal stalk sequences of NgR1 (Wen et al., 2005) are disrupted in chimera NgR1^{LRRCT}/NgR2^{stalk}, which may result in considerable structural alterations that reduce binding of MAG to the stalk of NgR2.

MAG binds to a 13 aa motif in the NgR2 stalk

To more directly address the importance of the NgR2 stalk for MAG binding, we generated the deletion mutant NgR2^{stalk}, lacking amino acid residues 1–314, which includes the entire LRR cluster (domains LRRNT-LRR-LRRCT). As shown in Figure 3, expression of the NgR2 stalk alone is sufficient to support MAG binding. Compared with wild-type NgR2, however, MAG binding to NgR2^{stalk} is reduced to 55 ± 7%. Moreover, deletion of 13 aa residues from the N terminus of the NgR2 stalk, including residues P315–S327, results in NgR2$^{stalk\Delta 13}$, a mutant that supports MAG binding poorly (9 ± 1%). Selective deletion of P315–S327 from full-length NgR2 (NgR2$^{\Delta P315–S327}$) decreases binding to 41 ± 11% compared with wild-type NgR2 (Fig. 3*B*). Of note, none of the receptor mutants examined showed preferential binding of MAG(1–5)-Fc over MAG(1–3)-Fc, confirming our observation that NgR1 and NgR2 complex with MAG independently of Ig4 and Ig5. Together, these results reveal that a 13 aa sequence motif (PTRPGSRARGNSS) within the NgR2 stalk, located proximal to the LRRCT-cap domain, harbors an important MAG-binding epitope. Because the 13 aa motif is not conserved in NgR1, our analysis provides a molecular explanation for the enhanced binding of MAG to NgR2 compared with NgR1.

The receptor deletion mutants NgR1$^{LRRCT+stalk}$ and NgR2$^{LRRCT+stalk}$ exhibit opposite activities in primary neurons

Thus far, our structural studies identified the deletion mutant NgR2$^{LRRCT+stalk}$ as the minimal receptor fragment that confers high-affinity MAG binding. MAG binding to NgR2$^{LRRCT+stalk}$ is enhanced compared with full-length NgR2. To ask whether NgR2$^{LRRCT+stalk}$ is sufficient to augment MAG inhibition if ectopically expressed in primary neurons (CGNs) (Venkatesh et al., 2005), we expressed NgR2$^{LRRCT+stalk}$ in P7 CGNs and assayed neurite outgrowth on CHO or CHO-MAG feeder cells (Fig. 3*C*). Interestingly, when cultured on CHO feeder cells, NgR2$^{LRRCT+stalk}$-expressing CGNs show significantly shorter neurites than eGFP-transfected or untransfected neurons. This suggests that NgR2$^{LRRCT+stalk}$ functions as a constitutively active receptor that leads to neurite outgrowth inhibition in the absence of MAG. NgR2$^{LRRCT+stalk}$-elicited neurite outgrowth is reversed in the presence of Y27632, suggesting that it occurs through activation of the RhoA-ROCK pathway (supplemental Fig. S5, available at www.jneurosci.org as supplemental material). When plated on CHO-MAG cells both eGFP and NgR2$^{LRRCT+stalk}$ are significantly inhibited compared with eGFP-transfected neurons plated on CHO cells. Because NgR2$^{LRRCT+stalk}$ inhibits growth independently of MAG, we wondered whether NgR1$^{LRRCT+stalk}$, the corresponding deletion mutant of NgR1, shows similar activity when expressed in CGNs. As shown in Figure 3*C*, NgR1$^{LRRCT+stalk}$ does not function as a constitutively active growth inhibitory receptor. On CHO feeder cells, neurite length of NgR1$^{LRRCT+stalk}$ or eGFP-transfected neurons was indistinguishable. Interestingly, NgR1$^{LRRCT+stalk}$ attenuates neurite outgrowth inhibition in CGNs plated on CHO-MAG feeder cells, suggesting that this construct has dominant negative activity. Neurite length of NgR1$^{LRRCT+stalk}$-expressing neurons is significantly increased compared with eGFP-transfected or nontransfected neurons. Together, these observations suggest that the LRRCT and stalk sequences of NgR1 and NgR2 have opposite activities when expressed in primary neurons. Thus, sequences C-terminal to the array of LRR$_{(1–8.5)}$ exhibit receptor-specific features and are emerging as important regulators of Nogo receptor function.

The stalk region of NgR1 attenuates Nogo-66 and OMgp binding

While the NgR1 LRR cluster (residues 27–310) is sufficient for Nogo-66, OMgp, and MAG binding (Fournier et al., 2002), we previously reported that the NgR1 stalk region influences Nogo-66 binding strength (Venkatesh et al., 2005). Here, we confirm and expand on this initial observation by showing that Nogo-66 and OMgp binding to NgR1 increases to 428 ± 50% and 601 ± 40% if the NgR1 stalk is replaced by the corresponding sequences of NgR2. Similarly, deletion of the NgR1 stalk (NgR1$^{\Delta stalk}$) leads to a significant increase in Nogo-66 and OMgp binding while MAG binding is largely unaltered (Venkatesh et al., 2005). The reason for the enhanced binding of Nogo-66 and OMgp to receptor variants lacking the NgR1 stalk is not known. One possibility is that the NgR1 stalk partially masks access to Nogo-66 and OMgp binding sites located within the NgR1 LRR cluster. To test this idea, deletion mutants lacking portions of the NgR1 stalk were generated (supplemental Table 1, available at www.jneurosci.org as supplemental material) and assayed for ligand binding. A 70 aa disulfide loop is formed between Cys^{266} and Cys^{335} of NgR1 which is further subdivided by intercalated disulfide loops located N-terminally (Cys^{264}–Cys^{287}) and

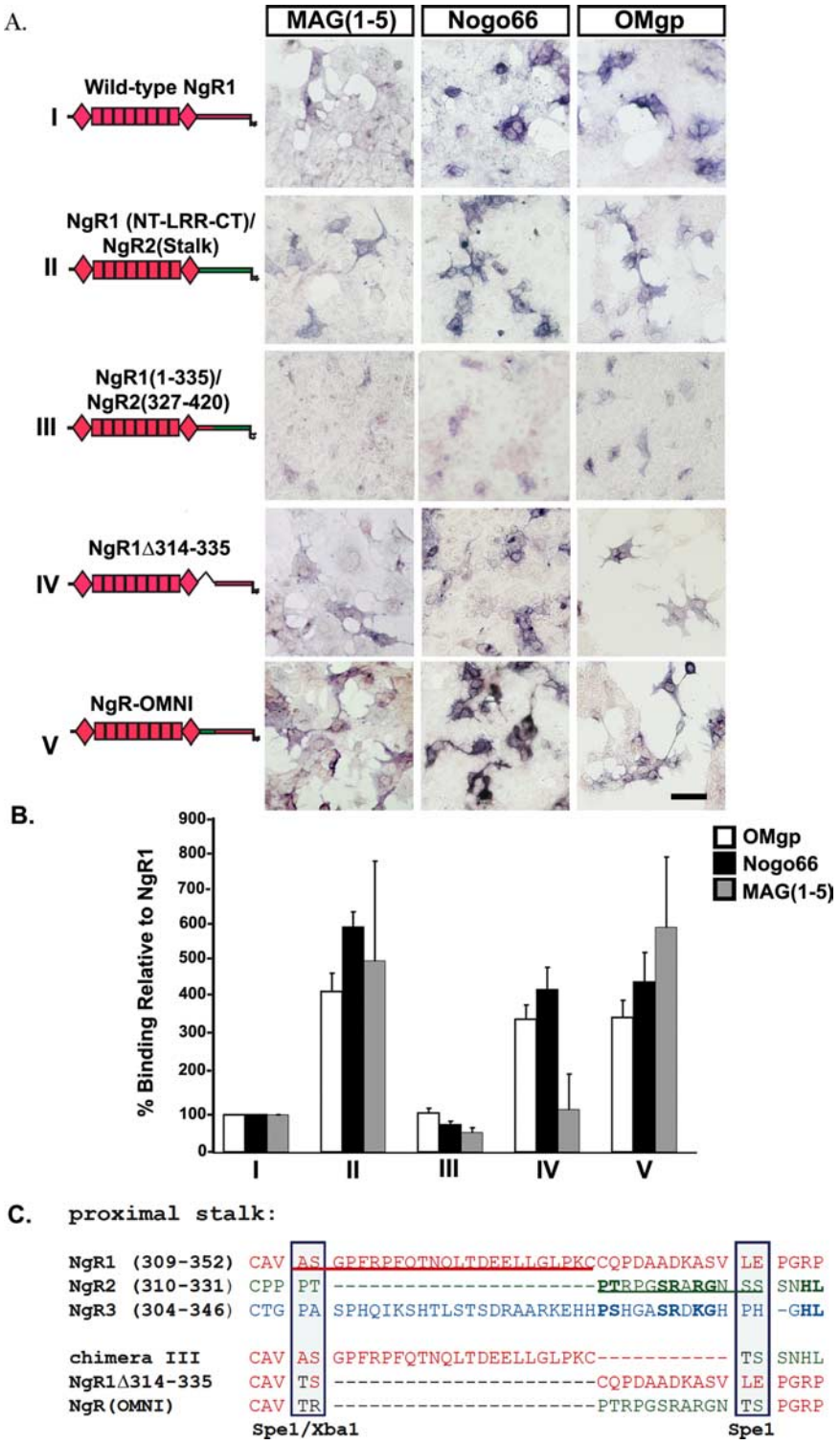

Figure 4. Development of NgR^{OMNI}, a receptor variant with enhanced ligand-binding properties. ***A***, Binding of MAG(1–5)-Fc [MAG(1–5)], AP-Nogo-66 [Nogo-66], and AP-OMgp [OMgp] to Nogo receptor variants. Compared with wild-type NgR1 (construct I), binding of MAG(1–5), Nogo-66, and OMgp to the chimeric receptor NgR1(NT-LRR-CT)/NgR2(stalk) (construct II) is greatly enhanced. The proximal stalk sequences of NgR1 (residues 314–335) are part of the cysteine loop formed between Cys309 and Cys335 and were found to be necessary (construct IV) and sufficient (construct III) to attenuate binding of Nogo-66 and OMgp to NgR1. Deletion of residues 314–348 of the proximal stalk region of NgR1 and simultaneous insertion of the 13 aa MAG-binding motif identified in the NgR2 stalk (residues 315–327) results in NgR^{OMNI}, a construct which combines the high-affinity binding properties of wild-type NgR1 toward Nogo-66 and OMgp with the high-affinity binding properties of wild-type NgR2 toward MAG. ***B***, Quantification of OMgp (white bars), Nogo-66 (black bars), and MAG(1–5)-Fc (gray bars) binding to receptor variants, normalized to wild-type NgR1. Ligand binding is shown in relative AP units. Error bars represent SEMs and are the result of at least four independent experiments. The interactions of NgR1 with OMgp, Nogo-66, and MAG were each arbitrarily set at 100%. ***C***, Sequence alignment of the proximal stalk regions of wild-type NgR1 (red; residues 309–352), wild-type NgR2 (green; residues 310–331), and wild-type NgR3 (yellow; residues 304–346). The NgR1 stalk region G314-C335 was found to partially attenuate or "mask" binding of Nogo-66 and OMgp to NgR1 and is underlined in red. The 13 aa residue MAG binding motif in the NgR2 stalk (P315–S327) is underlined in green. The NgR2 and NgR3 stalks show a weak degree of sequence conservation (conserved residues are shown in bold and were used as a means to align the proximal stalk sequences of the three Nogo receptors). Chimera III (NgR1(1–335)/NgR2(327–420) includes the "mask" but lacks the MAG-binding motif and supports inhibitor binding very similar to wild-type NgR1. Construct IV (NgR1Δ314–335) shows that deletion of residues 314–335 of the NgR1 stalk greatly enhances Nogo-66 and OMgp binding without affecting MAG(1–5)-Fc binding. The construct NgR(OMNI) lacks the NgR1 "mask region" and also includes the NgR2 MAG binding motif P315–S327, and as a result, confers high-affinity binding of all three myelin inhibitory ligands. The position of restriction enzyme sites (*Spe*I and *Xba*I) introduced to engineer these receptor mutants are shown in black. Scale bar, 30 μm.

C-terminally (Cys^{309}–Cys^{336}), resulting in a three bladed propeller-like structure, with the three blades being 23 (residues 264–287), 20 (residues 288–308), and 27 (residues 309–336) amino acids in length. Significantly, deletion of residues 314–335 in the disulfide loop formed between Cys^{309}–Cys^{336} of NgR1 (NgR1$^{\Delta 314-335}$) increases Nogo-66 binding to 354 ± 39% and OMgp binding to 433 ± 60% compared with wild-type NgR1 (100%). Of note, MAG binding to NgR1$^{\Delta 314-335}$ is not enhanced compared with wild-type NgR1 (Fig. 4). This suggests that the disulfide loop formed between Cys^{309}–Cys^{336} negatively influences Nogo-66 and OMgp binding to NgR1. To ask whether residues G314-C335 are sufficient to attenuate Nogo-66 and OMgp binding, we generated a chimeric receptor in which G314-C335 remained intact but the distal part of the NgR1 stalk (residues 336–473) was replaced by the corresponding sequences of NgR2 (chimera NgR1$^{1-335}$/NgR2$^{327-420}$). Similar to wild-type NgR1, Nogo-66 and OMgp binding to NgR1$^{1-335}$/NgR2$^{327-420}$ is attenuated compared with NgR1$^{\Delta 314-335}$ (Fig. 4*A*,*B*). This suggests that cysteine loop Cys^{309}–Cys^{336} of the NgR1 stalk is sufficient to partially block or "mask" access of Nogo-66 and OMgp to docking sites located on the concave face of the NgR1 LRR cluster.

Generation of NgR^{OMNI}, a receptor variant that exhibits enhanced binding of OMgp, MAG, and Nogo-66

The preceding results suggest that proximal stalk sequences of NgR1 (P314-C335) negatively regulate binding of Nogo-66 and OMgp to the NgR1 LRR cluster and that sequences in the proximal stalk region

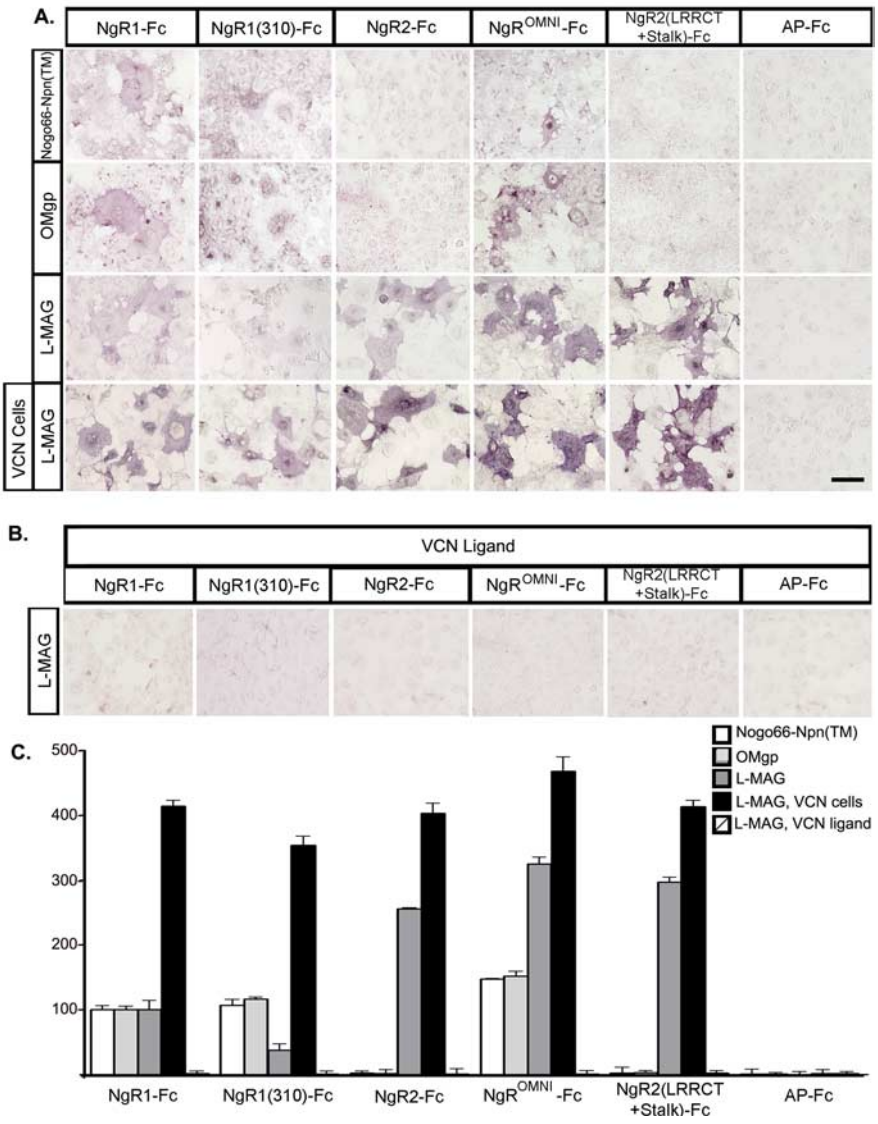

Figure 5. Soluble Nogo receptor variants show "reverse binding" to membrane-bound myelin inhibitors. ***A***, Nogo-66 fused to the transmembrane domain of Neuropilin-1 (Nogo-66-NpnTM), OMgp, and L-MAG were transiently expressed in COS-7 cells. For binding studies, Fc-tagged fusion proteins of Nogo receptor variants were oligomerized with an anti-human Fc antibody conjugated to AP. Consistent with "forward" binding studies, oligomerized NgR1-Fc, NgR1(310)-Fc, and NgR^{OMNI}-Fc bind to membrane-bound Nogo-66 and OMgp. NgR2-Fc, NgR2$^{LRRCT+stalk}$-Fc, and AP-Fc show no binding to Nogo-66-NpnTM) or OMgp. Importantly, NgR^{OMNI}-Fc binding to L-MAG is robust and comparable to NgR2-Fc and NgR2$^{LRRCT+stalk}$-Fc. Preincubation of L-MAG-expressing COS cells with VCN (VCN cells) to remove terminal sialic acid moieties, leads to significantly enhanced binding of all soluble receptors. Most notably, NgR1(310)-Fc binding increases nearly 10-fold. ***B***, Conversely, VCN-treatment of soluble Nogo receptors (VCN ligand) completely abrogates binding to L-MAG. ***C***, Quantification of "reverse" binding in relative AP units. Binding is normalized to the interactions of NgR1-Fc (100%) with Nogo-66-NpnTM (white bars), OMgp (light gray bars), and L-MAG (dark gray bars). Binding to desialylated L-MAG (VCN cells) is shown in black bars and binding of desialylated receptor fusion proteins (VCN, ligand) to L-MAG is shown in striped bars. AP-Fc was used as a control ligand. The error bars represent SEMs and were calculated from at least three independent sets of experiments. Scale bar, 30 μm.

of NgR2 (P315–S327) enhance the strength of the NgR2–MAG association. In an attempt to generate a chimeric receptor that combines the enhanced ligand-binding properties of NgR1$^{\Delta 314-335}$ toward Nogo-66 and OMgp with the strong binding of MAG toward NgR2, we removed the NgR1 "mask" (loop sequences A314–C335) and, in addition, replaced residues 336–349 of NgR1 by the 13 aa MAG-binding motif identified in the NgR2 stalk. The resulting chimera, NgR1$^{1-313}$/NgR2$^{315-327}$/NgR1$^{349-473}$, was then analyzed for ligand binding in COS cells. As shown in Figure 4, replacement of residues A314-C349 in NgR1 by residues N315-S327 of NgR2 does not result in a "masking" of Nogo-66 or OMgp binding sites. Similar to NgR1$^{\Delta 315-335}$, binding of Nogo-66 (359 ± 47%) and OMgp (455 ± 79%) to NgR1$^{1-313}$/NgR2$^{315-327}$/NgR1$^{349-473}$ is greatly enhanced compared with wild-type NgR1. Furthermore, NgR1$^{1-313}$/NgR2$^{315-327}$/NgR1$^{349-473}$ shows greatly enhanced MAG binding (600 ± 187%) compared with wild-type NgR1 (100%). MAG binding to NgR1$^{1-313}$/NgR2$^{315-327}$/NgR1$^{349-473}$ is enhanced 1.2-fold compared with wild-type NgR2. Thus, chimera NgR1$^{1-313}$/NgR2$^{315-327}$/NgR1$^{349-473}$ exceeds the ligand-binding properties of wild-type NgR1 toward Nogo-66 and OMgp, and combines it with the high-affinity MAG-binding properties of wild-type NgR2. Because of its greatly enhanced binding toward OMgp, MAG, and Nogo inhibitors of growth, chimera NgR1$^{1-313}$/NgR2$^{315-327}$/NgR1$^{349-473}$ was renamed NgR^{OMNI}.

Soluble Nogo receptors show "reverse binding" to membrane-bound inhibitors

The robust binding of NgR^{OMNI} to OMgp, Nogo-66, and MAG prompted us to explore whether a soluble variant of this receptor possesses MAG or CNS myelin antagonistic properties and how it compares to those previously reported for NgR(310)ecto, also known as NgR1(310)-Fc, in overcoming neurite outgrowth inhibition (Fournier et al., 2002). NgR1(310)-Fc is comprised of the dimerized NgR1 LRR cluster (residues 27–310) fused to the Fc region of human IgG1. In a first series of experiments, we assessed binding of soluble receptor variants to membrane-bound inhibitors. As shown in Figure 5*A*, NgR1(310)-Fc associates specifically with membrane-bound Nogo-66, OMgp, and L-MAG expressed in COS-7. Under similar conditions, soluble NgR2-Fc or AP-Fc fail to interact with membrane-bound Nogo-66 and OMgp, indicating that the weak binding observed with NgR1(310)-Fc is specific. Membrane-bound MAG (L-MAG) shows the following binding preference NgR^{OMNI}-Fc (325 ± 9%) > NgR2$^{CT+stalk}$-Fc (296 ± 8%) > NgR2-Fc (255 ± 2%) > NgR1-Fc (100%) > NgR1(310)-Fc (37 ± 10%) > AP-Fc (0%) (Fig. 5). Binding of soluble NgR^{OMNI}-Fc and NgR1(310)-Fc to membrane-bound Nogo-66 (147 ± 1% and 106 ± 9%, respectively) and OMgp (151 ± 8% and 116 ± 3%) at 100 nM is only modestly increased compared with NgR1-Fc (100%) and binding of NgR^{OMNI}-Fc to L-MAG is comparable to NgR2-Fc but nearly 10-fold stronger than for NgR1(310)-Fc (Fig. 5*A*,*B*). Thus, NgR^{OMNI}-Fc combines and exceeds the inhibitor-binding activities of NgR1-Fc and NgR2-Fc.

MAG homophilic and heterophilic interactions are sialic acid dependent

Previously, it was found that enzymatic removal of terminal sialic acids from MAG-expressing cells results in significantly enhanced binding of gangliosides or erythrocytes (Collins et al., 1997; Tropak and Roder, 1997; Cao et al., 2007). Commensurate with these reports, VCN treatment of L-MAG-expressing COS-7 cells, results in substantially enhanced binding of NgR1-Fc (4.1-fold), NgR2-Fc (1.6-fold), NgR2$^{LRRCT+stalk}$-Fc (1.4-fold), and NgR^{OMNI}-Fc (1.4-fold) compared with control L-MAG cells not treated with VCN (Fig. 5*A*,*B*). Most notably, binding of NgR1(310)-Fc to L-MAG increases nearly 10-fold from 37 ± 10% before VCN treatment to 354 ± 14% following VCN treatment. A control construct, AP-Fc, does not bind to membrane-bound L-MAG either before or after VCN treatment (Fig. 5*B*,*C*). The enhanced binding of soluble receptor variants to desialylated MAG cells suggests that terminal sialic acids on MAG itself, or on other cell surface glycans, compete with sialic acid moieties on soluble Nogo receptors for complex formation with the MAG lectin. Similar to the MAG-NgR1 and MAG-NgR2 heterophilic interactions, MAG homophilic binding is regulated in a sialic acid-dependent manner (supplemental Fig. S2, available at www.jneurosci.org as supplemental material). Together, these results suggest the existence of numerous carbohydrate ligands recognized by the MAG lectin, and similar to other siglecs, MAG function may be regulated by overall levels of *cis*- and *trans*-sialic acid associations (Varki and Angata, 2006).

Terminal sialic acids on *O*-linked glycans of the NgR2 stalk support MAG binding

Desialylation of soluble Nogo receptors fusions proteins, including NgR1-Fc, NgR1(310)-Fc, NgR2-Fc, NgR2$^{CT-stalk}$-Fc, and NgR^{OMNI}-Fc, completely abolishes binding to L-MAG-expressing COS-7 cells (Fig. 5). Moreover, a soluble form of the NgR2 stalk (NgR2^{stalk}-Fc) is sufficient to associate with L-MAG in a sialic acid-dependent manner (supplemental Fig. S6, available at www.jneurosci.org as supplemental material). The NgR2 stalk sequence harbors a consensus sequence for *N*-glycosylation, N325-S327 (NSS), that falls within the 13 aa region critical for MAG binding (Fig. 4*C*). To examine whether *N*-glycosylation at N325 is important for MAG binding, we generated NgR2$^{stalk(N325E)}$-Fc, a mutant defective for *N*-glycosylation. NgR2^{stalk}-Fc and NgR2$^{stalk(N325E)}$-Fc show comparable binding to L-MAG and binding of both fusion proteins is greatly enhanced following desialylation of L-MAG-expressing COS cells (supplemental Fig. S6, available at www.jneurosci.org as supplemental material). Because N325 is the only *N*-glycosylation consensus sequence in the NgR2 stalk, this suggests that *N*-glycosylation of the NgR2 does not contribute to MAG binding. Our data argue that terminal sialic acids associated with *O*-linked glycan structures are recognized by the MAG lectin.

Soluble NgR^{OMNI}-Fc has MAG antagonistic properties exceeding the ones previously reported for NgR1(310)-Fc

Because different neuronal cell types use different receptor systems to signal MAG inhibition, we compared the efficacy of soluble NgR1(310)-Fc and NgR^{OMNI}-Fc in overcoming MAG-elicited neurite outgrowth inhibition of E18 cortical neurons and P7–P8 cerebellar granule neurons (CGNs). For neurite outgrowth inhibition studies, MAG-Fc was adsorbed to nitrocellulose-coated glass coverslips and coated with laminin for CGNs or fibronectin for cortical neurons. Substrate-adsorbed MAG-Fc inhibits neurite outgrowth of P7–P8 CGNs and E18 cortical neurons in a dose-dependent manner (supplemental Fig. S7, available at www.jneurosci.org as supplemental material). Inhibition is MAG specific as it is reversed in the presence of a MAG function-blocking antibody (supplemental Fig. S7*E*, available at www.jneurosci.org as supplemental material).

Substrate-adsorbed MAG-Fc, but not siglec3-Fc, leads to a significant inhibition of neurite outgrowth of both cortical neurons and CGNs. Neurite length of CGNs is decreased to 65% on MAG-Fc compared with no ligand control or siglec-3 (Fig. 6) and neurite length of cortical neurons is decreased to 58% on MAG-Fc compared with no ligand control or siglec-3 (Fig. 6*B*,*D*). Bath application of soluble NgR^{OMNI}-Fc (10 μg/ml) but not NgR1(310)-Fc (10 μg/ml) leads to significantly enhanced neurite outgrowth of CGNs ($p < 0.005$) and cortical neurons ($p < 0.05$) cultured on substrate adsorbed MAG-Fc. Similar to NgR^{OMNI}-Fc, anti-MAG mAb513 promotes neurite outgrowth on substrate-bound MAG-Fc. Neither NgR1(310)-Fc nor NgR^{OMNI}-Fc influenced neurite outgrowth on control substrate (Fig. 6*B*,*D*). Together, these results demonstrate that in neurite outgrowth inhibition assays with two different types of primary neurons NgR^{OMNI}-Fc significantly attenuates MAG inhibition.

For a more detailed characterization of NgR^{OMNI}-Fc, we performed a dose–response experiment and also compared its efficacy to NgR1(310)-Fc in neutralizing MAG inhibition. Soluble receptors were added to the culture medium at a final concentration of 0–20 μg/ml. In addition, we compared the efficacy of these two fusion proteins to a soluble version of the minimal MAG receptor, NgR2$^{LRRCT+stalk}$-Fc (Fig. 7). We found that NgR^{OMNI}-Fc and NgR2$^{LRRCT+stalk}$-Fc, at a final concentration of 5 μg/ml (or higher), significantly enhance neurite outgrowth of E18 cortical neurons plated on MAG substrate ($p < 0.001$). Moreover, at 5 μg/ml or above both fusion proteins lead to significantly enhanced neurite length compared with NgR1(310)-Fc (Fig. 7*B*). Within the concentration range tested, NgR1(310)-Fc failed to significantly release MAG inhibition. Consistent with previous reports (Fournier et al., 2002; Zheng et al., 2005, He et al., 2003), however, we observed that NgR1(310)-Fc significantly attenuates inhibition of CGNs cultured on substrate-bound Nogo-66 (data not shown).

NgR^{OMNI}-Fc binds to endogenously expressed myelin inhibitor and blocks CNS myelin inhibition

From a therapeutic point of view, a more relevant question concerns the efficacy of NgR^{OMNI}-Fc in attenuating the growth inhibitory action of adult spinal cord myelin. To ask whether soluble receptors complex with endogenously expressed MAG, we performed affinity precipitation experiments with myelin extracts obtained from adult rat spinal cord tissue. Western blot analysis revealed the presence of Nogo-A, MAG, and OMgp in spinal cord myelin extracts (supplemental Fig. S8, available at www.jneurosci.org as supplemental material). MAG is enriched in the myelin membrane fraction compared with the microsomal fraction; Nogo-A, on the other hand, is enriched in the microsomal fraction compared with the myelin membrane fraction; and OMgp shows equal distribution between the two fractions (supplemental Fig. S8, available at www.jneurosci.org as supplemental material). As shown in Figure 8*A*, both NgR^{OMNI}-Fc and NgR2$^{LRRCT+stalk}$ form a complex with MAG present in spinal cord myelin. No interaction of NgR1(310)-Fc and MAG was detected. To assess whether soluble receptors associate with OMgp we used recombinant OMgp. Figure 8*B* shows that NgR^{OMNI}-Fc, NgR1-Fc, and NgR1(310)-Fc interact with OMgp, while NgR2$^{LRRCT+stalk}$-Fc does not. These results show that soluble

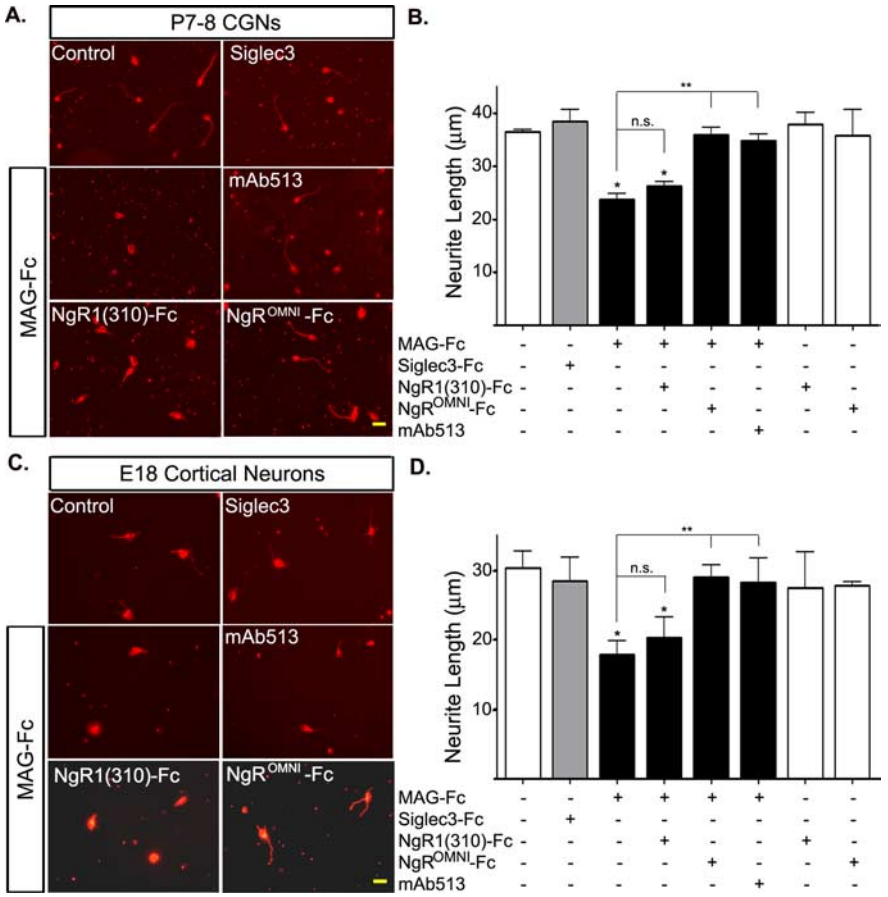

Figure 6. NgR^{OMNI}-Fc but not NgR1(310)-Fc significantly attenuates MAG inhibition of cortical and cerebellar neurons. ***A***, ***C***, Neurite outgrowth of P7–P8 rat cerebellar granule neurons (CGNs) (***A***) and E18 rat cortical neurons (***C***) is inhibited by substrate-bound MAG (Siglec-4), but not by Siglec-3. In the presence of NgR^{OMNI}-Fc (10 μg/ml) or the function-blocking antibody mAb513 (25 μg/ml), MAG inhibition is greatly attenuated. In contrast, NgR1(310)-Fc (10 μg/ml) does not lead to a significant release of MAG inhibition. For quantification of neurite length, cultures were fixed and immunolabeled with TuJ1. ***B***, ***D***, Neurite length of P7–P8 CGNs (***B***) and neurite length of E18 cortical neurons (***D***) on control substrate and on substrate-bound MAG-Fc in the presence or absence of NgR^{OMNI}-Fc and NgR1(310)-Fc. In the absence of MAG, neither NgR^{OMNI}-Fc nor NgR1(310)-Fc influences neurite outgrowth. For CGNs, 45–278 neurites were measured per condition for each of three independent assays. *$p < 0.001$ compared with control; **$p < 0.005$ compared with MAG-Fc only; n.s., not statistically significant. For cortical neurons, 15–262 neurites were measured per condition for each of three independent assays. Results are presented as the mean ± SEM. *$p < 0.05$ compared with control; **$p < 0.05$ compared with MAG-Fc only (unpaired *t* test). Scale bar, 10 μm.

NgR^{OMNI}-Fc interacts with soluble myelin inhibitors. Consistent with binding experiments to membrane-associated inhibitors expressed in COS-7 cells, NgR^{OMNI}-Fc, but not NgR1(310)-Fc, supports strong binding of endogenously expressed MAG.

Similar to neurite outgrowth experiments on substrate-bound MAG-Fc, we assayed NgR^{OMNI}-Fc and NgR1(310)-Fc for overcoming neurite outgrowth inhibition of CNS myelin. When plated on myelin substrate, neurite outgrowth is decreased to 61% for CGNs and 66% for cortical neurons. Myelin does not completely abolish neurite outgrowth, as in our assays we use low concentrations of laminin or fibronectin, growth-promoting ECM molecules which can partially override myelin inhibition (David et al., 1995; Laforest et al., 2005). Soluble NgR^{OMNI}-Fc significantly attenuates myelin inhibition ($p < 0.05$), while NgR1(310)-Fc and control human IgG do not release inhibition (Fig. 8). There is a dose-dependent trend for NgR1(310)-Fc to overcome myelin inhibition of CGNs (p value 0.22) and cortical neurons (p value 0.26) in this experimental paradigm, but the increase in neurite length is not statistically significant. As shown in Figure 8*A*, NgR1(310)-Fc does not complex with spinal cord myelin derived MAG in an affinity precipitation experiment. Because the spinal cord myelin isolated for our studies is rich in MAG (supplemental Fig. S8, available at www.jneurosci.org as supplemental material), this may explain why NgR1(310)-Fc does not lead to a significant release of growth inhibition. Other myelin inhibitors such as Nogo-A and OMgp, however, are also present in detergent extracts of spinal cord myelin used for growth inhibition experiments (supplemental Fig. S8*B*, available at www.jneurosci.org as supplemental material). Together, our results reveal that in a direct comparison NgR^{OMNI}-Fc is superior to NgR1(310)-Fc in overcoming CNS myelin mediated neurite outgrowth inhibition *in vitro*.

Discussion

Molecular analysis of the myelin inhibitor interactions with the Nogo receptor family members NgR1 and NgR2 identified specific sequence motifs that either positively or negatively influence complex formation and receptor function. Insights gained from these studies enabled the development of NgR^{OMNI}-Fc, a chimeric NgR1/NgR2 construct that supports OMgp, MAG, and Nogo binding with greater affinity than wild-type NgR1 or NgR2. NgR^{OMNI}-Fc complexes with membrane-bound and soluble inhibitors in a nonproductive manner and antagonizes their neurite outgrowth inhibitory activity. In the presence of NgR^{OMNI}-Fc, MAG- or spinal cord myelin-elicited neurite outgrowth inhibition of cortical and cerebellar neurons is significantly decreased.

The growth inhibitory site of MAG does not directly bind to NgR1 or NgR2

The first three Ig-like domains of the MAG ectodomain are sufficient to support binding of NgR1 and NgR2. In marked contrast, domains Ig3–5 of MAG fail to associate with NgR1 or NgR2. Functional studies with substrate-adsorbed MAG ectodomain deletion constructs revealed that the bulk of MAG inhibitory activity is associated with MAG(3–5)-Fc, a finding consistent with a previous report showing that a MAG inhibitory site is located in domain Ig5 (Cao et al., 2007). A trend toward decreased neurite length was found when neurons were cultured on substrate adsorbed MAG(1–3)-Fc, however, neurite length was not significantly shorter when compared with control cultures. Consistent with this observation, neurite length of P5 CGNs cultured on CHO control cells or CHO cells stably expressing membrane-bound MAG(1–3) is virtually identical (Cao et al., 2007). Thus, we conclude that the Nogo receptor binding site in the MAG ectodomain is distinct from the site that signals growth inhibition.

Implications for Nogo receptor function

The molecular dissection of the MAG ectodomain into a NgR1 and NgR2 binding fragment (Ig1–3) and a growth inhibitory

fragment (Ig3–5) is consistent with previous studies demonstrating that *NgR1* wild-type and mutant neurons are strongly and similarly inhibited when cultured on CHO-MAG feeder cells or substrate adsorbed membranes of CHO-MAG cells (Chivatakarn et al., 2007; Venkatesh et al., 2007; Williams et al., 2008). Because P7 CGNs do not express NgR2 (Venkatesh et al., 2005), studies with *NgR1* null CGNs imply the existence of NgR1- and NgR2-independent mechanism(s) for MAG to bring about growth inhibition.

In 2- to 3-week-old DRG neurons, *NgR1* is required for the acute growth cone-collapsing effects of MAG, Nogo-66, and OMgp, but not for the ability to inhibit neurite outgrowth when presented as substrates (Kim et al., 2004; Zheng et al., 2005; Chivatakarn et al., 2007). How do the present findings fit with previous observations that the growth cone-collapsing activity and substrate growth-inhibitory activities of MAG can be mechanistically dissociated? A first possibility is that NgR1 functions as a high-affinity ligand-binding component of a MAG holoreceptor complex that upon binding of MAG(1–3) presents the MAG inhibitory site in Ig5 to a signal-transducing receptor component. If the affinity of MAG(3–5) for its receptor is lower than the one of MAG(1–3) for NgR1, and the concentration of soluble MAG limiting in the collapse assay but saturating when presented in membrane-bound form on the surface of CHO-MAG cells, loss of *NgR1* would reduce responsiveness to soluble MAG-Fc but not to membrane-bound L-MAG. Alternatively, distinct and independent mechanisms may be used for NgR1 ligand-elicited growth cone collapse and substrate inhibition.

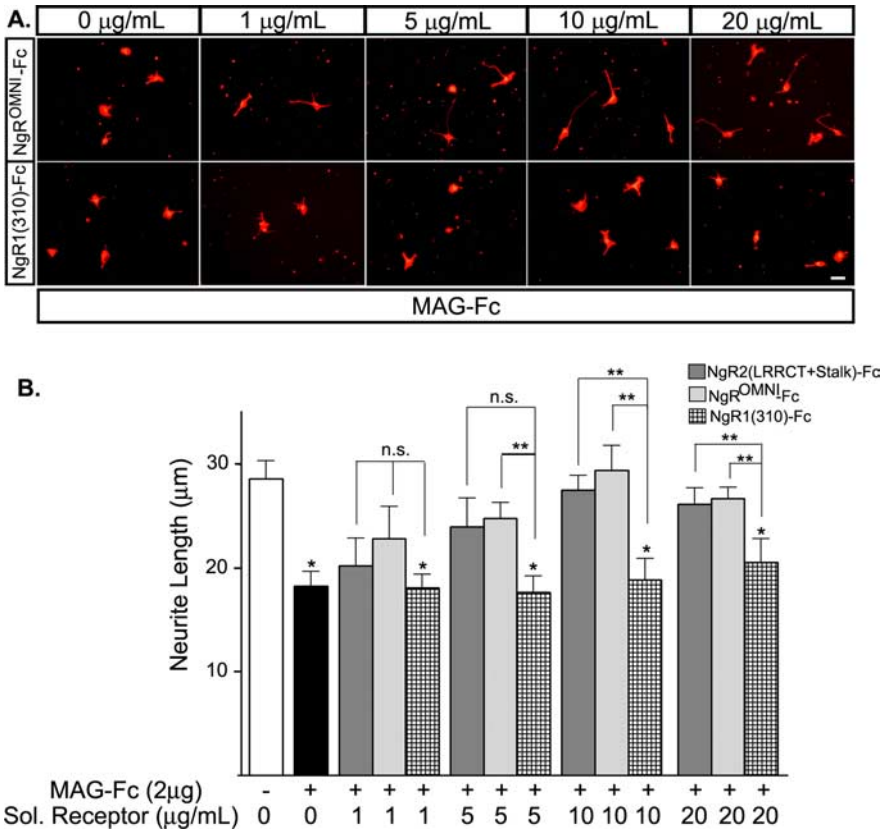

Figure 7. Dose–response curve of MAG antagonism with NgR^{OMNI}-Fc. ***A***, E18 cortical neurons were plated on substrate-coated MAG-Fc (2 μg per well). Increasing doses (0–20 μg/ml final concentration) of soluble NgR^{OMNI}-Fc, NgR2$^{LRRCT+stalk}$-Fc (data not shown), or NgR1(310)-Fc were added to the cultures. For quantification of neurite length cultures were immunolabeled with TuJ1. ***B***, Quantification of neurite length revealed that NgR^{OMNI}-Fc (light gray) and NgR2$^{LRRCT+stalk}$-Fc (dark gray) both overcome MAG inhibition in a dose-dependent manner. NgR1(310)-Fc (checkerboard) does not lead to a significant release of MAG inhibition at any of the concentrations tested. Data presented are the result of four independent assays; 18–264 neurites were measured per condition for each assay. Results are presented as the mean ± SEM. *$p < 0.05$, significantly different from neurons grown on control substrate; **$p < 0.05$ significantly different from cultures growth in the presence of NgR(310)-Fc (unpaired *t* test). Scale bar, 10 μm.

While this manuscript was under revision, paired-Ig receptor B (PirB) was identified as a neuronal receptor for MAG, Nogo, and OMgp (Atwal et al., 2008). Similar to *NgR1*−/− DRG neurons, *PirB*−/− DRG neurons are resistant to MAG-, Nogo-66-, and OMgp-elicited growth cone collapse. Importantly, functional ablation of PirB results in a partial but significant release of neurite outgrowth inhibition on substrate-bound Nogo-66, MAG, OMgp, and CNS myelin. On myelin but not Nogo66 substrate, functional ablation of NgR1 and PirB simultaneously, leads to further increased neurite outgrowth. It will be interesting to explore whether PirB binds directly to MAG(1–3)-Fc or MAG(3–5)-Fc, and to what extent such interactions contribute to growth inhibitory responses in different types of neurons. Elucidating the precise mechanisms of how PirB and Nogo receptors collaborate in neuronal inhibition will require additional studies.

Mechanism of NgR^{OMNI}-Fc-elicited neurite outgrowth

If NgR1 is not necessary for neurite outgrowth inhibition on substrate-adsorbed MAG and neither NgR1 nor NgR2 binds to Ig(5) of MAG, how does soluble NgR^{OMNI}-Fc promote neurite outgrowth in the presence of MAG or CNS myelin? A first possibility is that soluble NgR^{OMNI}-Fc complexed with MAG sterically hinders the proper association of the MAG inhibitory site in Ig(5) with a signal-transducing component of the neuronal MAG holoreceptor. Alternatively, soluble NgR^{OMNI}-Fc may bind to additional components of the MAG holoreceptor and thereby impair the proper assembly of a functional receptor complex. Though NgR1 has been reported to undergo homophilic binding (Fournier et al., 2002), the MAG and myelin antagonistic effects of NgR^{OMNI}-Fc are likely independent of an association with neuronal NgR1. This is primarily based on the observation that NgR1 is a nonessential receptor component for MAG-, Nogo-66-, OMgp-, and CNS myelin-elicited longitudinal neurite outgrowth inhibition. Moreover, it has been found that NgR1(310)-Fc promotes neurite outgrowth in the presence of Nogo-66 in an *NgR1*-independent manner (Zheng et al., 2005). Finally, because NgR^{OMNI}-Fc binds to MAG in a sialic acid-dependent manner, NgR^{OMNI}-Fc is expected to block interactions of MAG not only with NgR1 and NgR2, but also with β1-integrin and gangliosides, including GT1b and GD1a. Simultaneous loss of multiple MAG binding partners has recently been reported to substantially release MAG inhibition (Mehta et al., 2007; Venkatesh et al., 2007), suggesting the existence of multiple and at least partially redundant neuronal MAG receptor systems, several of which may simultaneously be blocked by NgR^{OMNI}-Fc.

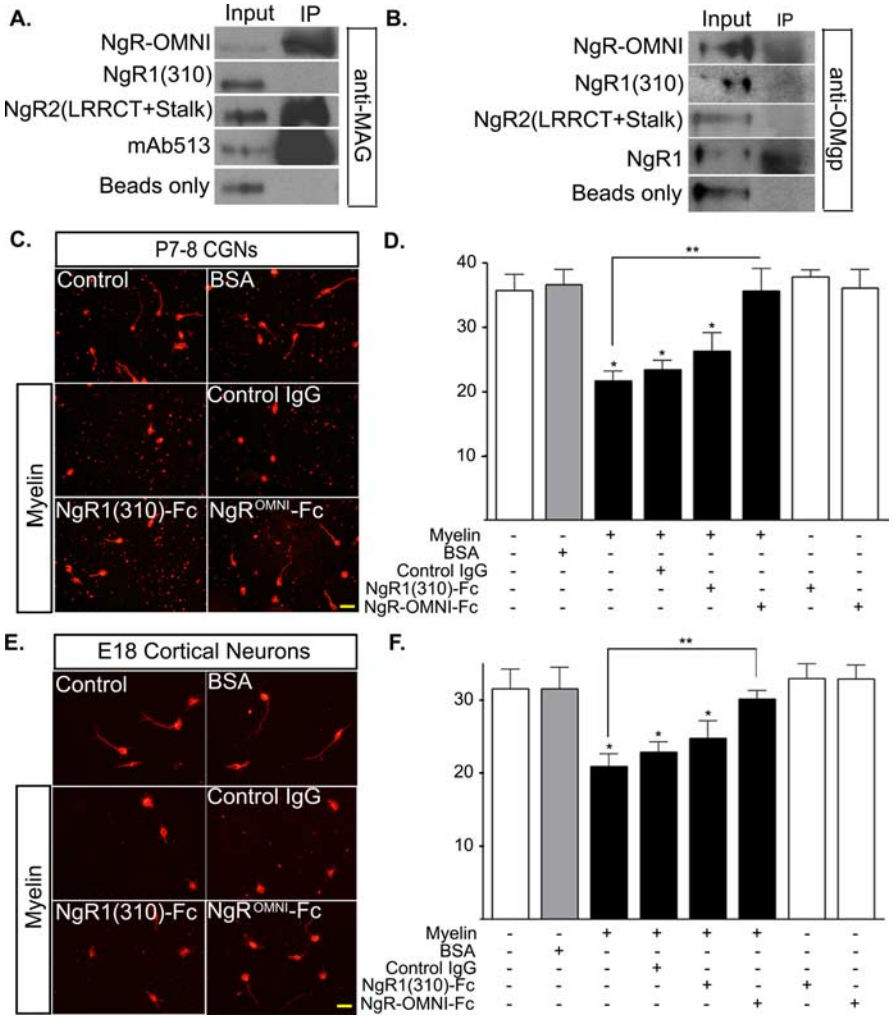

Figure 8. NgR^{OMNI}-Fc overcomes spinal cord myelin inhibition of neurite outgrowth. ***A***, Affinity precipitation studies revealed that NgR^{OMNI}-Fc, but not NgR1(310)-Fc, binds strongly to MAG endogenously expressed in adult rat spinal cord myelin. Similar to NgR^{OMNI}-Fc, the deletion construct NgR2$^{LRRCT+stalk}$-Fc forms a complex with endogenously expressed MAG. As positive and negative controls, pull-down experiments with anti-MAG (mAb513) or beads only are shown. ***B***, Affinity precipitation studies also showed an interaction between recombinant OMgp-His and NgR^{OMNI}-Fc, NgR1(310)-Fc, and NgR1-Fc but not NgR2$^{LRRCT+stalk}$-Fc. ***C***, ***E***, P7–P8 rat CGNs (***C***) and E18 cortical neurons (***E***) were cultured on glass coverslips coated with poly-D-lysine and either laminin (CGNs) or fibronectin (cortical neurons). In the presence of substrate-bound spinal cord myelin but not control protein (BSA), neurite outgrowth is significantly inhibited. Bath application of soluble NgR^{OMNI}-Fc (10 μg/ml) CGNs ($p < 0.05$) and cortical neurons ($p < 0.05$) but not NgR1(310)-Fc (10 μg/ml) (CGNs, $p = 0.22$) or cortical neurons ($p = 0.26$) myelin inhibition is significantly attenuated. For quantification of neurite length cultures were immunolabeled with TuJ1. ***D***, ***F***, Neurite length of CGNs (***D***) and cortical neurons (***F***) on control substrate versus myelin in the presence of NgR^{OMNI}-Fc and NgR1(310)-Fc. In the absence of myelin (white bars), neither NgR^{OMNI}-Fc nor NgR1(310)-Fc influences baseline neurite outgrowth. For CGNs, 63–323 neurites were measured per condition for each of three independent assays. *$p < 0.05$ compared with control; **$p < 0.05$ compared with myelin only. For cortical neurons, 14–365 neurites were measured per condition for each of at least three independent assays. Results are presented as the mean ± SEM. *$p < 0.05$ compared with control; **$p < 0.05$ compared with myelin only (unpaired *t* test). Scale bar, 10 μm.

In a direct comparison, NgR^{OMNI}-Fc was found to be more potent than NgR1(310)-Fc in overcoming MAG and CNS myelin inhibition. The most significant difference between NgR^{OMNI}-Fc and NgR1(310)-Fc is the nearly 10-fold increased binding of MAG. In previous studies NgR1(310)-Fc has been shown to significantly attenuate myelin inhibition *in vitro* (Fournier et al., 2002; Liu et al., 2002), however, some of these experiments were performed with chick DRG neurons or NgR1(310)-Fc was presented by mixing the protein with the inhibitory substrate (Fournier et al., 2002; Liu et al., 2002; Zheng et al., 2005). In the current study, soluble receptor fusion proteins were directly added to the culture medium, which may more closely model the use of NgR^{OMNI}-Fc as a therapeutic agent *in vivo*.

NgR1 and NgR2 are *N*- and *O*-linked sialoglycoproteins

NgR1 and NgR2 support MAG binding in an α2,3-neuraminidase-sensitive manner. Whether NgR1 and NgR2 themselves are sialoglycoproteins that directly complex with the MAG lectin activity, or whether MAG binding occurs more indirectly through an association with gangliosides, has not yet been fully resolved (Venkatesh et al., 2005; Williams et al., 2008). Here, we revisited this issue and found that NgR1 and NgR2 from *Galgt1* heterozygous and mutant brains show a similar decrease in molecular weight following VCN treatment. Studies with glycosidases revealed that NgR1 and NgR2 carry *N*-linked and *O*-linked sialoglycoconjugates. Soluble NgR1-Fc and NgR2-Fc fusion proteins show sialic acid-dependent binding to membrane-bound L-MAG. Sialic acid moieties on carbohydrates of the NgR1 LRR cluster and on *O*-linked glycans of the NgR2 stalk participate in MAG binding. Additional evidence for the importance of proper receptor glycosylation stems from the observation that NgR2-Fc derived from Sf9 insect cells fails to support L-MAG binding (personal communication between M. Semavina, D. Nikolov, L.A.R., and R.J.G.). Desialylated NgR1-Fc and NgR2-Fc fail to complex with membrane-bound L-MAG and binding cannot be restored by exogenously added GT1b (data not shown). Together these experiments would argue against a direct involvement of gangliosides in a NgR1–MAG or NgR2–MAG recognition complex. Weak interactions, such as the sialic acid-dependent binding of GT1b to a "KFGR" motif in NgR1, however, can formally not be ruled out (Williams et al., 2008).

General features of the NgR2–MAG recognition complex

Several crystal structures of complexed LRR proteins have been resolved, revealing general principles of LRR-mediated protein recognition. Ligands approach the LRR cluster from the concave side to engage in multivalent and high-affinity protein–protein interactions (Kobe and Deisenhofer, 1995; Huizinga et al., 2002). The NgR1-ligand interactions occur on the concave face of the LRR cluster and conform with the general rules of LRR-containing protein complexes (Laurén et al., 2007). Our mutagenesis study revealed that MAG binds to at least two distinct and dissociable sites on NgR2, each of which is sufficient to independently support MAG binding. One site is located within the NgR2 LRRCT-cap, and a second site that binds MAG with higher affinity is located within

a 13 aa motif of the NgR2 stalk region. Thus, the NgR2–MAG complex seems to form an exception to the general rule of LRR protein ligand interactions, as the LRRNT-cap and LRR(1–8.5) domains are dispensable for high-affinity ligand binding. The bulk of MAG binding is mediated by a short sequence motif located in the NgR2 stalk, outside of the NgR2 LRRNT-LRR-LRRCT cluster. Future studies will be needed to determine whether NgR2 forms a complex with one MAG molecule (1:1) through the engagement of two different sites, similar to glycoprotein Ibα (GpIbα) and vWF (Huizinga et al., 2002), or whether NgR2 is capable of supporting binding of two MAG molecules (1:2), similar to the GpIbα complex with thrombin (Celikel et al., 2003; Dumas et al., 2003).

Deletion of a 20 aa region within cysteine loop 309–335 of NgR1 leads to a significant increase in Nogo-66 and OMgp binding. This suggests that the proximal stalk region of NgR1 partially blocks access of Nogo-66 and OMgp to the NgR1 LRR cluster. Residues 309–335 of NgR1 may undergo posttranslational modification(s) or participate in NgR1 homophilic or heterophilic *cis*-interactions, and, as a result, partially mask access of Nogo-66 and OMgp to receptor docking sites.

In addition to regulating ligand binding strength, the C-terminal sequences of NgR1 and NgR2 participate in receptor function. Deletion of the NgR1 stalk results in a receptor variant with dominant negative activity toward Nogo-66, MAG, and OMgp (Domeniconi et al., 2002; Fournier et al., 2002). Here, we identify the deletion mutant NgR2$^{LRRCT+stalk}$ as the minimal NgR2 receptor sufficient to confer high-affinity MAG binding. Functional studies in primary neurons further revealed that NgR2$^{LRRCT+stalk}$ behaves as a constitutively active inhibitory receptor whereas NgR1$^{LRRCT+stalk}$ has dominant negative activity and partially attenuates MAG inhibition. Thus, sequences C-terminal to LRR$_{(1-8.5)}$ harbor receptor-specific features and are emerging as important regulators of Nogo receptor function.

NgR^{OMNI}-Fc, a novel tool to overcome CNS myelin inhibition

Antibody-based strategies and soluble receptor ectodomains that directly bind and neutralize myelin inhibitors have been used successfully to promote neurite outgrowth *in vitro* (Caroni and Schwab, 1988; Fournier et al., 2002) and regenerative axonal growth following spinal cord injury *in vivo* (Bregman et al., 1995; Huang et al., 1999; Li et al., 2004; Wang et al., 2006). Whether complexing of myelin inhibitors with antibodies or Fc-fusion proteins simply neutralizes their inhibitory activity or also leads to enhanced clearance of myelin debris is not well understood (Vargas and Barres, 2007). While exact mechanisms await further elucidation, these studies validate the concept that acute antagonism of myelin inhibitors following spinal cord injury promotes anatomical and functional repair in rodents. We developed and characterized NgR^{OMNI}-Fc, a soluble receptor variant that associates strongly with the prototypic myelin inhibitors OMgp, MAG, and Nogo-66. Because of its superior binding and inhibitor neutralizing properties over NgR1(310)-Fc *in vitro*, NgR^{OMNI}-Fc is emerging as a promising new tool that warrants further development to examine its potential to overcome myelin inhibition following CNS injury *in vivo*. Finally, new roles for NgRs and their ligands in immune system function (David et al., 2008), synaptic plasticity (Lee et al., 2008), and neurodegeneration (Park and Strittmatter, 2007) may significantly expand the therapeutic opportunities of NgR^{OMNI}-Fc.

References

Atwal JK, Pinkston-Gosse J, Syken J, Stawicki S, Wu Y, Shatz C, Tessier-Lavigne M (2008) PirB is a functional receptor for myelin inhibitors of axonal regeneration. Science 322:967–970.

Barton WA, Liu BP, Tzvetkova D, Jeffrey PD, Fournier AE, Sah D, Cate R, Strittmatter SM, Nikolov DB (2003) Structure and axon outgrowth inhibitor binding of the Nogo-66 receptor and related proteins. EMBO J 22:3291–3302.

Bregman BS, Kunkel-Bagden E, Schnell L, Dai HN, Gao D, Schwab ME (1995) Recovery from spinal cord injury mediated by antibodies to neurite growth inhibitors. Nature 378:498–501.

Cafferty WB, Strittmatter SM (2006) The Nogo-Nogo receptor pathway limits a spectrum of adult CNS axonal growth. J Neurosci 26:12242–12250.

Cao Z, Qiu J, Domeniconi M, Hou J, Bryson JB, Mellado W, Filbin MT (2007) The inhibition site on myelin-associated glycoprotein is within Ig-domain 5 and is distinct from the sialic acid binding site. J Neurosci 27:9146–9154.

Caroni P, Schwab ME (1988) Antibody against myelin-associated inhibitor of neurite growth neutralizes nonpermissive substrate properties of CNS white matter. Neuron 1:85–96.

Celikel R, McClintock RA, Roberts JR, Mendolicchio GL, Ware J, Varughese KI, Ruggeri ZM (2003) Modulation of alpha-thrombin function by distinct interactions with platelet glycoprotein Ib alpha. Science 301:218–221.

Chivatakarn O, Kaneko S, He Z, Tessier-Lavigne M, Giger RJ (2007) The Nogo-66 receptor NgR1 is required only for the acute growth cone-collapsing but not the chronic growth-inhibitory actions of myelin inhibitors. J Neurosci 27:7117–7124.

Collins BE, Kiso M, Hasegawa A, Tropak MB, Roder JC, Crocker PR, Schnaar RL (1997) Binding specificities of the sialoadhesin family of I-type lectins. Sialic acid linkage and substructure requirements for binding of myelin-associated glycoprotein, Schwann cell myelin protein, and sialoadhesin. J Biol Chem 272:16889–16895.

Colman DR, Kreibich G, Frey AB, Sabatini DD (1982) Synthesis and incorporation of myelin polypeptides into CNS myelin. J Cell Biol 95:598–608.

David S, Braun PE, Jackson DL, Kottis V, McKerracher L (1995) Laminin overrides the inhibitory effects of peripheral nervous system and central nervous system myelin-derived inhibitors of neurite growth. J Neurosci Res 42:594–602.

David S, Fry EJ, López-Vales R (2008) Novel roles for Nogo receptor in inflammation and disease. Trends Neurosci 31:221–226.

Domeniconi M, Cao Z, Spencer T, Sivasankaran R, Wang K, Nikulina E, Kimura N, Cai H, Deng K, Gao Y, He Z, Filbin M (2002) Myelin-associated glycoprotein interacts with the Nogo66 receptor to inhibit neurite outgrowth. Neuron 35:283–290.

Dumas JJ, Kumar R, Seehra J, Somers WS, Mosyak L (2003) Crystal structure of the GpIbalpha-thrombin complex essential for platelet aggregation. Science 301:222–226.

Filbin MT (2003) Myelin-associated inhibitors of axonal regeneration in the adult mammalian CNS. Nat Rev Neurosci 4:703–713.

Fournier AE, Gould GC, Liu BP, Strittmatter SM (2002) Truncated soluble Nogo receptor binds Nogo-66 and blocks inhibition of axon growth by myelin. J Neurosci 22:8876–8883.

Giger RJ, Venkatesh K, Chivatakarn O, Raiker SJ, Robak L, Hofer T, Lee H, Rader C (2008) Mechanisms of CNS myelin inhibition: evidence for distinct and neuronal cell type specific receptor systems. Restor Neurol Neurosci 26:97–115.

Goh EL, Young JK, Kuwako K, Tessier-Lavigne M, He Z, Griffin JW, Ming GL (2008) beta1-integrin mediates myelin-associated glycoprotein signaling in neuronal growth cones. Mol Brain 1:10.

He XL, Bazan JF, McDermott G, Park JB, Wang K, Tessier-Lavigne M, He Z, Garcia KC (2003) Structure of the Nogo receptor ectodomain: a recognition module implicated in myelin inhibition. Neuron 38:177–185.

Hofer T, Tangkeangsirisin W, Kennedy MG, Mage RG, Raiker SJ, Venkatesh K, Lee H, Giger RJ, Rader C (2007) Chimeric rabbit/human Fab and IgG specific for members of the Nogo-66 receptor family selected for species cross-reactivity with an improved phage display vector. J Immunol Methods 318:75–87.

Huang DW, McKerracher L, Braun PE, David S (1999) A therapeutic vaccine approach to stimulate axon regeneration in the adult mammalian spinal cord. Neuron 24:639–647.

Huizinga EG, Tsuji S, Romijn RA, Schiphorst ME, de Groot PG, Sixma JJ, Gros P (2002) Structures of glycoprotein Ib alpha and its complex with von Willebrand factor A1 domain. Science 297:1176–1179.

Kawai H, Allende ML, Wada R, Kono M, Sango K, Deng C, Miyakawa T, Crawley JN, Werth N, Bierfreund U, Sandhoff K, Proia RL (2001) Mice expressing only monosialoganglioside GM3 exhibit lethal audiogenic seizures. J Biol Chem 276:6885–6888.

Kelm S, Pelz A, Schauer R, Filbin MT, Tang S, de Bellard ME, Schnaar RL, Mahoney JA, Hartnell A, Bradfield P, Crocker PR (1994) Sialoadhesin, myelin-associated glycoprotein and CD22 define a new family of sialic acid-dependent adhesion molecules of the immunoglobulin superfamily. Curr Biol 4:965–972.

Kim JE, Liu BP, Park JH, Strittmatter SM (2004) Nogo-66 receptor prevents raphespinal and rubrospinal axon regeneration and limits functional recovery from spinal cord injury. Neuron 44:439–451.

Kobe B, Deisenhofer J (1995) A structural basis of the interactions between leucine-rich repeats and protein ligands. Nature 374:183–186.

Laforest S, Milanini J, Parat F, Thimonier J, Lehmann M (2005) Evidences that beta1 integrin and Rac1 are involved in the overriding effect of laminin on myelin-associated glycoprotein inhibitory activity on neuronal cells. Mol Cell Neurosci 30:418–428.

Laurén J, Hu F, Chin J, Liao J, Airaksinen MS, Strittmatter SM (2007) Characterization of myelin ligand complexes with neuronal Nogo-66 receptor family members. J Biol Chem 282:5715–5725.

Lee H, Raiker SJ, Venkatesh K, Geary R, Robak LA, Zhang Y, Yeh HH, Shrager P, Giger RJ (2008) Synaptic function for the Nogo-66 receptor NgR1: regulation of dendritic spine morphology and activity-dependent synaptic strength. J Neurosci 28:2753–2765.

Li S, Liu BP, Budel S, Li M, Ji B, Walus L, Li W, Jirik A, Rabacchi S, Choi E, Worley D, Sah DW, Pepinsky B, Lee D, Relton J, Strittmatter SM (2004) Blockade of Nogo-66, myelin-associated glycoprotein, and oligodendrocyte myelin glycoprotein by soluble Nogo-66 receptor promotes axonal sprouting and recovery after spinal injury. J Neurosci 24:10511–10520.

Liu BP, Fournier A, GrandPré T, Strittmatter SM (2002) Myelin-associated glycoprotein as a functional ligand for the Nogo-66 receptor. Science 297:1190–1193.

Liu BP, Cafferty WB, Budel SO, Strittmatter SM (2006) Extracellular regulators of axonal growth in the adult central nervous system. Philos Trans R Soc Lond B Biol Sci 361:1593–1610.

McGee AW, Yang Y, Fischer QS, Daw NW, Strittmatter SM (2005) Experience-driven plasticity of visual cortex limited by myelin and Nogo receptor. Science 309:2222–2226.

Mehta NR, Lopez PH, Vyas AA, Schnaar RL (2007) Gangliosides and Nogo receptors independently mediate myelin-associated glycoprotein inhibition of neurite outgrowth in different nerve cells. J Biol Chem 282:27875–27886.

Meyer-Franke A, Tropak MB, Roder JC, Fischer P, Beyreuther K, Probstmeier R, Schachner M (1995) Functional topography of myelin-associated glycoprotein. II. Mapping of domains on molecular fragments. J Neurosci Res 41:311–323.

Park JH, Strittmatter SM (2007) Nogo receptor interacts with brain APP and Abeta to reduce pathologic changes in Alzheimer's transgenic mice. Curr Alzheimer Res 4:568–570.

Schimmele B, Plückthun A (2005) Identification of a functional epitope of the Nogo receptor by a combinatorial approach using ribosome display. J Mol Biol 352:229–241.

Schnaar RL, Collins BE, Wright LP, Kiso M, Tropak MB, Roder JC, Crocker PR (1998) Myelin-associated glycoprotein binding to gangliosides. Structural specificity and functional implications. Ann N Y Acad Sci 845:92–105.

Schwab ME (1993) Experimental aspects of spinal cord regeneration. Curr Opin Neurol Neurosurg 6:549–553.

Strenge K, Schauer R, Kelm S (1999) Binding partners for the myelin-associated glycoprotein of N2A neuroblastoma cells. FEBS Lett 444:59–64.

Tang S, Shen YJ, DeBellard ME, Mukhopadhyay G, Salzer JL, Crocker PR, Filbin MT (1997) Myelin-associated glycoprotein interacts with neurons via a sialic acid binding site at ARG118 and a distinct neurite inhibition site. J Cell Biol 138:1355–1366.

Tropak MB, Roder JC (1997) Regulation of myelin-associated glycoprotein binding by sialylated cis-ligands. J Neurochem 68:1753–1763.

Vargas ME, Barres BA (2007) Why is Wallerian degeneration in the CNS so slow? Annu Rev Neurosci 30:153–179.

Varki A, Angata T (2006) Siglecs—the major subfamily of I-type lectins. Glycobiology 16:1R–27R.

Venkatesh K, Chivatakarn O, Lee H, Joshi PS, Kantor DB, Newman BA, Mage R, Rader C, Giger RJ (2005) The Nogo-66 receptor homologue NgR2 is a sialic acid-dependent receptor selective for myelin-associated glycoprotein. J Neurosci 25:808–822.

Venkatesh K, Chivatakarn O, Sheu SS, Giger RJ (2007) Molecular dissection of the myelin-associated glycoprotein receptor complex reveals cell type-specific mechanisms for neurite outgrowth inhibition. J Cell Biol 177:393–399.

Vinson M, Strijbos PJ, Rowles A, Facci L, Moore SE, Simmons DL, Walsh FS (2001) Myelin-associated glycoprotein interacts with ganglioside GT1b. A mechanism for neurite outgrowth inhibition. J Biol Chem 276:20280–20285.

Walmsley AR, McCombie G, Neumann U, Marcellin D, Hillenbrand R, Mir AK, Frentzel S (2004) Zinc metalloproteinase-mediated cleavage of the human Nogo-66 receptor. J Cell Sci 117:4591–4602.

Wang X, Baughman KW, Basso DM, Strittmatter SM (2006) Delayed Nogo receptor therapy improves recovery from spinal cord contusion. Ann Neurol 60:540–549.

Wen D, Wildes CP, Silvian L, Walus L, Mi S, Lee DH, Meier W, Pepinsky RB (2005) Disulfide structure of the leucine-rich repeat C-terminal cap and C-terminal stalk region of Nogo-66 receptor. Biochemistry 44:16491–16501.

Williams G, Wood A, Williams EJ, Gao Y, Mercado ML, Katz A, Joseph-McCarthy D, Bates B, Ling HP, Aulabaugh A, Zaccardi J, Xie Y, Pangalos MN, Walsh FS, Doherty P (2008) Ganglioside inhibition of neurite outgrowth requires Nogo receptor function: identification of interaction sites and development of novel antagonists. J Biol Chem 283:16641–16652.

Xie F, Zheng B (2008) White matter inhibitors in CNS axon regeneration failure. Exp Neurol 209:302–312.

Yang LJ, Zeller CB, Shaper NL, Kiso M, Hasegawa A, Shapiro RE, Schnaar RL (1996) Gangliosides are neuronal ligands for myelin-associated glycoprotein. Proc Natl Acad Sci USA 93:814–818.

Yiu G, He Z (2006) Glial inhibition of CNS axon regeneration. Nat Rev Neurosci 7:617–627.

Zheng B, Atwal J, Ho C, Case L, He XL, Garcia KC, Steward O, Tessier-Lavigne M (2005) Genetic deletion of the Nogo receptor does not reduce neurite inhibition in vitro or promote corticospinal tract regeneration in vivo. Proc Natl Acad Sci U S A 102:1205–1210.